REPUBLIC OF TURKEY

ADANA ALPARSLAN TÜRKEŞ SCIENCE AND TECHNOLOGY UNIVERSITY

GRADUATE SCHOOL OF NATURAL AND APPLIED SCIENCES

DEPARTMENT OF MECHANICAL ENGINEERING

SANDWICH PANEL PRODUCTION WITH LAYERED PRODUCTION TECHNOLOGY AND OPTIMIZATION

ONUR SELEK

MASTER OF SCIENCE

ADANA 2022

REPUBLIC OF TURKEY

ADANA ALPARSLAN TÜRKEŞ SCIENCE AND TECHNOLOGY UNIVERSITY

GRADUATE SCHOOL OF NATURAL AND APPLIED SCIENCES

DEPARTMENT OF MECHANICAL ENGINEERING

SANDWICH PANEL PRODUCTION WITH LAYERED PRODUCTION TECHNOLOGY AND OPTIMIZATION

ONUR SELEK

MASTER OF SCIENCE

SUPERVISOR

Asst. Prof. Dr. CEM BOĞA

ADANA 2022

I hereby declare that all information in this thesis has been obtained and presented in accordance with academic rules and ethical conduct. I also declare that, as required by these rules and conduct, I have fully cited and referenced all information that is not original to this work.

[İmza]
Onur SELEK

ABSTRACT

SANDWICH PANEL PRODUCTION WITH LAYERED PRODUCTION TECHNOLOGY AND OPTIMIZATION

Onur SELEK
Department of Mechanical Engineering
Supervisor: Asst. Prof. Dr. Cem BOĞA
September 2022, 63 pages

In this study, pure ABS (Acrylonitrile Butadiene Styrene) filament and 1%, 2%, 3%, 5% $CaCO_3$ nanoparticle added ABS filaments were produced. Sandwich panel cores in honeycomb geometry were produced with a double extruder 3D printer using filaments produced in different mixing ratios. Then, sandwich panel outer surfaces were produced from composite material by vacuum infusion method using carbon fiber fabric and epoxy. The produced core and composite outer surfaces were combined using structural adhesive and test specimens in the form of sandwich panels were obtained. Tensile test specimens, 3-point bending test specimens and compression test specimens were produced from the produced filaments. These samples were applied tensile test, 3-point bending test and compression test. The effects of nanoparticle additives on the strength properties of sandwich panels were investigated with the applied tests. In addition, numerical analysis was performed using the finite element method. The data obtained from the analysis and the results obtained from the experiments were compared. As a result of this study, it was observed that the $CaCO_3$ additive ratio directly affects the strength. It has been observed that the $CaCO_3$ additive added to ABS plastic up to the level of 3% increases the strength, while the material added after 3% decreases the strength due to the increase in brittleness.
Keywords: Nanocomposite sandwich panel, Vacuum infusion method, Tensile test, Three point bending test, Finite element analysis

ÖZET

KATMANLI ÜRETİM TEKNOLOJİSİ İLE SANDVİÇ PANEL ÜRETİMİ VE OPTİMİZASYONU

Onur SELEK
Makine Mühendisliği Anabilim Dalı
Danışman: Dr. Öğr. Üyesi Cem BOĞA
Eylül 2022, 63 sayfa

Bu çalışmada, saf ABS (Akrilonitril Bütadien Stiren) filament ve %1, %2, %3, %5 oranlarında $CaCO_3$ nano partükül katkılı ABS filamentler üretilmiştir. Farklı karışım oranlarında üretilmiş filamentler kullanılarak çift ektruderli 3 boyutlu (3D) yazıcı ile balpeteği geometrisinde sandviç panel çekirdekleri üretilmiştir. Daha sonra karbon fiber kumaş ve epoksi kullanılarak vakum infüzyon yöntemi ile sandviç panel dış yüzeyleri kompozit malzemeden üretilmiştir. Üretilen çekirdek ve kompozit dış yüzeyler yapısal yapıştırıcı kullanarak birleştirilip sandviç panel formunda test numuneleri elde edilmiştir. Üretilen filamentlerden çekme test numunleri, 3 nokta eğme testi numunmeleri ve basma testi numuneleri üretilmiştir. Bu numunelere çekme testi, 3 nokta eğme testi ve basma testi uygulanmıştır. Uygulanan testler ile nanopartükül katkısının sandviç panellerin dayanım özellikleri üzerine etkisi incelenmiştir. Ayrıca sonlu elemanlar metodu kullanılarak numerik analiz yapılmıştır. Analizden elde edilen veriler ile deneylerden elde edilen sonuçlar karşılaştırılmıştır. Bu çalışma sonucunda $CaCO_3$ katkı oranının mukavemeti doğrudan etkilediği görülmüştür. ABS plastiğe %3 seviyesine kadar eklenen $CaCO_3$ katkısının mukavemeti arttırdığı, %3'ten sonra eklenen ise malzemenin kırılganlığının artması nedeniyle mukavemetini azalttığı görülmüştür.

Anahtar Kelimeler: Nanokompozit sandviç panel, Vakum infüzyon yöntemi, Çekme testi, Üç nokta eğme testi, Sonlu elemanlar analizi

Dedication to my wonderful family for their endless love, support and encouragement, and to my supervisor, Asst. Prof. Dr. Cem BOĞA who always supported and motivated me during this process.

ACKNOWLEDGEMENTS

I would first like to thank my thesis supervisor, Asst. Prof. Dr. Cem BOĞA, Department of Mechanical Engineering, Faculty of Engineering, Adana Alparslan Türkeş Science and Technology University, for his noble guidance, his valuable suggestions, support with full encouragement and motivating guidance.

This thesis was financially supported by Department of Scientific Research Projects with project number of 20332003.

TABLE OF CONTENTS

LIST OF FIGURES

LIST OF TABLES

NOMENCLATURE

FRP	:	Fiber Reinforced Plastic, Fiber Reinforced Plastic
CFRP	:	Carbon Fiber Reinforced Plastic, Carbon Fiber Reinforced Plastic
MPa	:	Megapascal
GPa	:	Gigapascal
UV	:	Ultraviolet
SLA	:	Stereolithography
DLP	:	Digital Light Processing,
FDM	:	Fused Deposition Modeling, Fused Deposition Modeling
SLS	:	Selective Laser Sintering, Selective Laser Sintering
SLM	:	Selective Laser Melting, Selective Laser Melting
CPA	:	Electronic Beam Melting,
LOM	:	Laminated Object Manufacturing
BJ	:	Binder jetting
CAD	:	Computer Aided Design
STL	:	Standard triangle language, Standard triangle language
PEEK	:	Poly Ether-Ether Ketone
ABS	:	Acrylonitrile Butadiene Styrene
PLA	:	Polylactic Acid
PC	:	Polycarbonate
PMMA	:	Polymethylmethacrylate
HIPS	:	High impact polystyrene
PETG	:	Polyethylene terephthalate glycol
TPU	:	Thermoplastic polyurethane
CPE	:	Chlorinated polyethylene
PVA	:	Polyvinyl acrylic
PA	:	Polyamide
mm	:	millimeter
N	:	Newton

1. INTRODUCTION

1.1. Sandwich panels

Sandwich panels (Figure 1.1.) are widely used in sectors such as automotive, aerospace and construction. The most important criteria in composite sandwich panels are strength, weight and cost. Therefore, it is of great importance to strengthen the core and outer surfaces of sandwich panels, which are used in many areas, with reinforcement material. Traditional methods used in the production of core parts of sandwich structures cause design restrictions (Banhart, 2008), (Davalos, 2001). (Sharaf, 2011).

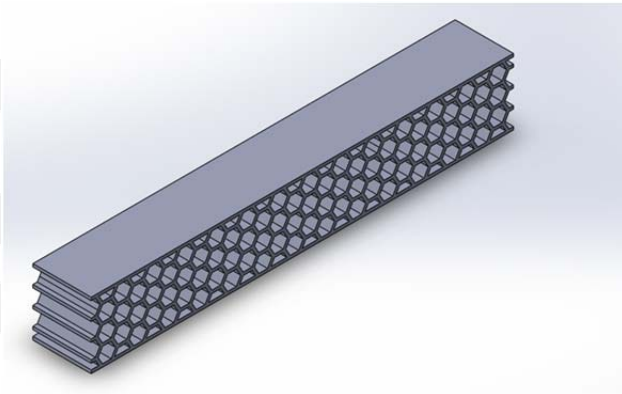

Figure 1.1. Sandwich panel

Sandwich construction and honeycomb structures developed in nature long before humans began to create structures and buildings. Many other examples can be found in the skeletal structures of plant and animal organisms, in the leaves of plants, as well as in the wing structures of birds. The honey bee's honeycomb is a structure with optimal material efficiency. It is created by two physical phenomena that each solve minimization tasks:

1. Hexagonal closest cylinder packing
2. Minimization of the surface energy

The hexagonal comb of the honey bee has been admired since ancient times and has inspired questions and reflections ever since (Nazzi, 2016). Sandwich elements are among the most important lightweight composite structures. Therefore, these elements are used in numerous industries such as aerospace, racing and mechanical engineering. A sandwich panel basically consists of an inner core of low stiffness and low density surrounded by two outer layers. These elements are bonded together with special structural adhesives or a resin system of the outer layers. There are many different possible combinations of core and cover layers. In this article, however, special attention is paid to cover layers made of carbon or glass fiber, in short CFRP and GRP, in conjunction with different types of core materials. In addition, the advantages and disadvantages of sandwich construction are explained in more detail. In the manufacture of carbon sandwich elements, core materials are particularly important because they represent the largest area in the sandwich section. There is a wide variety of possible core materials. Nomex and metal honeycombs or closed-cell foams such as Rohacell or Airex are mainly used in carbon components produced using autoclave technology (Flores-Johnson, 2010).

In terms of weight, honeycomb cores have the highest compressive strength of all support materials and very good resistance to chemicals, impact, vibration and fatigue. They are very flexible and therefore well suited for components with spherical curves. In principle, two types of honeycomb are used in the production of prepreg (prepreg = semi-finished product with pre-impregnated textile fiber matrix), Nomex or aluminum honeycomb. Nomex is a nylon-like aramid polymer produced in flame retardant and paper sheet form. Due to its low flammability and very low density, Nomex sandwich panels are widely used in aviation exterior cladding as well as aircraft cabin parts (Ahmad, 2020). In comparison, aluminum honeycombs have a slightly higher basis weight. As a result, higher loads can be absorbed with those. Due to the contact corrosion, aluminum honeycombs are usually only used in combination with glass fiber prepregs. The two honeycomb structures are manufactured using a similar process. To do this, several layers of paper or sheet metal are placed on top of each other and glued at the junction points with adhesive lines. These glue lines are offset with each layer, so that when the glue bundle is stretched, the typical honeycomb pattern becomes visible. To ensure the desired sandwich thickness, the bundle is cut into "slices" after gluing and the honeycombs are then stretched out. Closed-cell foams are generally used as an alternative to honeycomb cores. When it comes to prepreg components, a PMI foam such as Rohacell is mainly used. It is mainly characterized by its high resistance to pressure and temperature, which is very important for the curing process in the autoclave. Another advantage of foam cores is that they can be milled or thermally formed into almost any shape, making it possible to produce complex geometries (Wang, 2010). Various carbon structures are often subjected to bending loads in their function. The cover layers carry bending moments as tensile and compressive stresses in the longitudinal direction, while the core layer absorbs transverse forces as shear stresses.

Another advantage of sandwich elements is that the panels can be pre-manufactured in various formats and thicknesses. These sandwich panels can then be cut to desired shape using CNC milling. From these panel components, very solid structures can be created using snap or screw connections, similar to furniture construction, without the need to make special tools for this. Of course, there are also disadvantages that the use of sandwich panels can bring along. For example, the cover layers can be more easily separated from the core during impact events. Due to the open cell honeycomb structure, moisture can also enter the composite after damage has occurred. Additionally, if the design is incorrect, the sandwich elements tend to "bump" under high compressive loads, which means the sandwich core collapses (Li, 2005).

A sandwich always consists of two rigid top layers that absorb mainly stress and shear loads in the plane, and a light and pressure-resistant core that separates the top layers for high bending stiffness. When processing carbon sandwich components in the autoclave, cores made primarily of Nomex and aluminum honeycomb cores as well as closed-cell foams are used. Sandwich panels can be used in many industries and, due to their low mass, make a significant contribution to reducing the weight of the components (Li, 2005).

Sandwich elements as materials are not only found in construction. On the contrary: They are already much more widespread in other production areas - for example in automotive and shipbuilding, where lightweight constructions are in great demand for obvious reasons. In the building sector, light sandwich panels with metallic cover layers are primarily used for wall or roof constructions. This "industrial look" is no coincidence, because lightweight metal construction with sandwich panels is actually widespread in industrial buildings such as factory buildings or warehouses. Other typical areas of application are commercial buildings such as offices or hardware and technology stores (O'Hegarty, 2020).

In the construction of industrial halls, sandwich panels are also used as the only material for the entire building envelope. Since cover layers made of sheet metal are vapour-tight, with this type of construction it must be ensured with the help of suitable ventilation technology that condensation does not constantly form on the wall side facing the room. In many other construction projects, however, sandwich panels are not used as load-bearing outer wall elements, but only as additional cladding materials - for example in the form of facade panels. The cover layers do not always have to be made of metal, they can also be made of (reinforced) concrete , as is the case with panel construction. Or the composite element consists of three different materials. For example, a structure with concrete, insulating material and clinker is commonfor the facade (Georgescu, 2014), (Hipke, 2014).

As the name suggests, sandwich panels are constructed in a similar way to a sandwich: two galvanized sheet steel outer shells enclose a rigid foam core. Since the layers are very strongly connected to each other, they are also called Composite plates. The two sheet steel outer shells are protected against corrosion thanks to the galvanizing. The insulation material inside the two metal sheets provides high stability and durability to the sandwich panel, while at the same time it is light. But these are not the only advantages that sandwich panels achieve. Other advantages (Ding, 2013) it provides are:

- High load capacity
- Strong resilience
- Thermal insulation
- Sound insulation
- Easy to use

In addition, it is costly and takes a long time to change the processes from the design of the product to the mass production stage, to produce test samples with traditional methods. But the 3D printer allows the designer to design without thinking about the question of how to produce the model and to produce according to the needs. 3D printers take their place among modern production techniques because of the low cost and fast production of new designs, test samples and new prototypes with 3D printers. The main purpose of this thesis is to produce, test and analyze nanoparticle doped sandwich panels that are advantageous in terms of strength, weight and cost, and to optimize using the test data. In addition, by developing a numerical method, experimental application is not required in future tests (Ahmed, 2021).

1.2. Composites

Composites are combinations of two or more material components. This gives composite material additional properties that are not available individually. Ideally, the negative properties of the respective materials neutralize each other. The base material is modified according to the requirements and combined with other materials. If there is a special material requirement not found in the standard design, composite material is the right choice. The additive included in the composite should reinforce the advantages of the material. A composite material should reinforce the advantages of the composite.

In composite materials, the material components are referred to as "matrix" and "reinforcement". While the materials in alloys and polymers form an inseparable connection with one another, the individual substances are retained in composite materials. However, the structure is usually no longer visible to the naked eye.

Composites are divided into four categories:

- Fiber composite materials
- Particle composite materials
- Layered composite materials
- Penetrating Composites (Gibson, 2010).

A practical example of composite materials is their use in Formula 1. The material requirements there relate to two properties: the safety of the driver and the speed of the vehicle.

In racing, speed also depends on weight, among other things. This is one reason that has contributed to the development of the composite material carbon. Carbon is a carbon fiber reinforced plastic from which the chassis in racing are made. The composite material is very light and at the same time very stable (Savage, 2008), (Savage, 2010).

Further application examples for composite materials:

- Beverage packaging
- Swimming pools
- Structural engineering (Chauhan, 2022).

Composite materials are required for certain areas of application not only in high-performance sports, but also in everyday life. For example, the materials are used in advertising displays. A few decades ago, such signs were still made of wood. The material is much lighter than metal and can be painted by hand. However, wood is not weatherproof. In addition, digital printing has replaced manual painting. Composite materials offer the optimal solution for this.

One goal of composite materials is always to reinforce the advantages of the respective composite. This not only applies to weight, but also to corrosion and chemical resistance, electrical and thermal insulation and many other properties (Abbood, 2021). Composite materials, and especially fiber-reinforced polymers, have become an independent material group over the past 60 years, leaving a special niche of high-performance materials. New applications such as the BMW i3 or A350 from Airbus define the image and show a clear direction towards consistent lightweight technologies in larger quantities (Starke, 2016), (Marsh, 2010). An important success factor for composite materials is also the political environment and the changing attitude of society towards the protection of natural resources and the environment. Here, due to its excellent lightweight construction potential, composite materials on their own contribute to sustainability and conservation of resources. Although the polymers, fibers, computational methods and process technologies used to develop and manufacture fiber-plastic composites have not fundamentally changed in the last 10 years, this thesis reveals that there are still significant new developments. Due to the growing interest of the automotive industry, the chemical industry has also reinvented composite materials as a new growth market, leading to related material optimization and a certain expansion of polymer variants. But perhaps the most important advances have taken place in the field of machining. In addition to the continuing trend of developing new and highly specialized processes, aspects such as full automation, quality assurance and large series are becoming increasingly important. Manufacturers have a wide variety of process options to choose from. These range from manual laying processes to partially automated processes and fully automated systems in the sense of direct processing of polymer and fiber into complex components. Following the guiding principle of resource efficiency, trends are evolving both in starting materials through the use of bio-based polymers and natural fibers, and through holistic design and process development.

New research results on structural optimization or long-term behavior, as well as the increased use of process simulation, are leading to more efficient processes and products. In addition to the obvious potential and future challenges, there are currently certain operational hurdles that need to be overcome. First and foremost is the production costs of composite materials. However, the cost focus is also on starting materials, and here especially on the still relatively expensive carbon fibers and high-performance polymers. Established manufacturing processes, their material and process-technical foundations, process definition and a strong practical relevance are still in focus (Smith, 2006), (Zhang, 2021).

1.3. 3D printers

Additive Manufacturing (AM) – translated additive manufacturing (process), was defined by the ASTM (2012) as "a process of joining materials to make objects from 3D model data, usually layer upon layer, as opposed to subtractive manufacturing methodologies" Additive manufacturing processes differ from the traditional molding and subtractive production paradigms. With subtractive methods, a raw material is processed by means of the action of removing force such as milling, turning, drilling or spark erosion in order to create a desired geometry. Forming processes create the geometry through the application of mechanical or thermal forces such as those used in bending, pressing and casting. Additive processes, on the other hand, create the geometry by adding, applying and depositing material through physical or chemical hardening or melting processes. In addition, under the term hybrid methodsall other procedures are described that either cannot be clearly categorized or combine several paradigms. By generating geometries based on digital 3D model data, additive manufacturing can also be classified as a digital production process. Digital production processes differ from electrical, mechanical and manual processes, but at the same time build on their technical achievements. From a technical point of view, additive manufacturing processes are also forming processes, but do not require any special tools such as molds. The geometry is based on digital 3D model data (Wohlers, 2012), (Gupta, 2012).

Additive manufacturing processes describe digital production technologies that correspond to the additive production paradigm. They are always electrically operated and generate a desired geometry based on digital 3D data. The correct general term for the process at the production paradigm level is "additive manufacturing", which can be translated as "additive manufacturing process". The level of production paradigms does not yet describe a technical type of realization or an area of application (Lim, 2012).

While in the past models and prototypes were created manually, automated production processes are often used today. Instead of making models by hand using cardboard and foam or modeling design drafts out of clay, templates for production are now often produced with the aid of computers. This saves time and money in product development. As early as 1984, Chuck Hull (founder of 3D Systems) developed the first additive process, stereolithography, and commercialized it a few years later. In the years that followed, further processes such as 3DP and FDM were developed, all of which were protected by patents. Initially, the methods were mainly used to create inexpensive prototypes for product development using rapid prototyping. While the requirements for durability, quality and stability were not particularly high at the beginning due to the use as demonstration models, the quality has improved over the years through constant improvements to the machines and new materials, as well as with the help of powerful hardware and computer technology. Some processes could now produce objects that not only fulfilled the function of prototypes but could also be used as a finished end product. The boundary between the prototype and the finished end product became ever narrower and the term rapid manufacturing and direct manufacturing were coined (Su, 2018).

Although the technologies have been around for a long time, there has been a real boom in rapid manufacturing systems in recent years. Several circumstances can be considered as an explanation. Expiration of the patent for the Fused Deposition Modeling (FDM) process: A few years ago, the patent for the FDM printing process expired and enabled the creation of the open source 3D printer (RepRap Irwin 2014).

Better access and broader understanding of computer systems: Due to the advancing computerization in recent decades, computer systems and the associated (3D) software have gained an increasing number of users. The inhibitions and fears of contact with computers and new technologies have decreased as a result. Price reduction and technical development of 3D printing systems: Due to greater demand, better technology and "new" developments, additive manufacturing systems have become increasingly affordable and interesting. Above all, the open hardware project RepRap triggered a real boom in inexpensive home -made 3D printers and made the devices affordable for private households. Emergence of 3D service providers: The relatively high costs of professional AM systems also led to a centralization of such machines in the form of production parks. Some companies make the services available not only to industry, but also to private customers as an online service. The first 3D printing service providers emerged. This made 3D printing accessible to small businesses and private users (Su, 2018), (RepRap Irwin, 2014).

Interest on the part of politicians and investors : Recently, this technology has also experienced support from politicians and investors. Governments of various countries (including China, USA , UK and EU) see additive production forms as an opportunity to bring production back into their own country , save wage costs or increase innovative strength. Projects and research related to AM have been and are funded by the public sector and private investors. The areas of application often run across sectors, industries and areas and are now not just limited to the manufacturing industry (Tofail, 2018).

Areas in which AM technologies are already being used (sometimes still experimental):

- Medicine (bioprinting for tissue engineering, implants, prostheses, dentistry, models for the preparation of operations and manufacturing of hearing aids)
- Science and research (in the form of nanoprinting, bioprinting and space projects)
- Art, fashion and jewelery production (textiles, jewellery, casting templates for precious metal jewellery)
- Aerospace (for creating lightweight and high-strength parts)
- Production: especially in product development, prototyping, tool making
- Food sector (currently still very experimental)
- Construction industry (contour crafting) (with the aim of printing entire buildings)

In addition, such systems are also enjoying increasing interest in the hobby, hobbyist, model making, consumer and private sectors, as well as increasing use in small companies and start-ups for the production of small series (Revilla-León, 2020), (Najmon, 2019), (Godoi, 2016).

1.4. Calsium Carbonate

Calcium carbonate is a chemical compound of the elements calcium , carbon and oxygen with the chemical formula $CaCO_3$. As a carbonate, it is a calcium salt of carbonic acid and, in the solid state, consists of an ion lattice with C_2+ ions and CO_3 2-ions in a ratio of 1:1. Calcium carbonate is one of the most widespread compounds on earth, primarily in the form of sedimentary rocks. Calcium carbonate occurs primarily in the form of the minerals calcite and aragonite. Another modification of $CaCO_3$ is the mineral vaterite, which precipitates in the form of microscopically small crystals, particularly from supersaturated solutions. Calcium carbonate is a main component in marble, limestone and dolomite, it is found in the exoskeleton of crustaceans, corals, mussels, snails and protozoa. The first limestones of noteworthy dimensions were formed by stromatolites more than two billion years ago. Contrary to popular belief, the bones and teeth of vertebrates do not contain calcium carbonate, but the substances hydroxyapatite (in the bones), which also contain calcium, and additionally fluorapatite in the teeth. Calcium carbonate itself is hardly soluble in pure water. However, in the presence of dissolved carbon dioxide, the solubility increases more than 100-fold. The weathering of limestone is based on this effect, whereby the easily soluble calcium hydrogen carbonate $Ca(HCO_3)_2$ is formed. Because of its solubility, calcium hydrogen carbonate is a component of most natural waters, in varying concentrations depending on the rock. Calcium carbonate is also dissolved by other acidic components in the air and by nitrification in the soil. Most of the natural deposits of calcium carbonate owe their formation to the reversal of this dissolving process, i. e. the removal of carbonic acid through an increase in temperature. In nature, calcium carbonate forms a variety of rocks that are chemically identical but differ in a number of ways. It is precipitated by introducing carbon dioxide into milk of lime (calcium hydroxide) and thus obtained as a precipitate:

$$CaCO_3 \longrightarrow CaO + CO_2 \quad (1)$$

$$CaO+H_2O \longrightarrow Ca(OH)_2 \quad (2)$$

$$Ca(H)_2+CO_2 \longrightarrow CaCO_3+H_2O \quad (3)$$

Synthetic calcium carbonate is referred to as PCC (precipitated calcium carbonate) – in contrast to GCC (ground calcium carbonate) (Al Omari, 2016).

The precipitation takes place at a solids content of about 20%. Different crystal modifications (crystal morphologies) can be produced via the process control (temperature, concentration), preferably rhombohedral or scalenohedral crystal form. Because it is possible to work with high-purity starting products, the PCCs are particularly white and also have advantages in terms of opacity. In the meantime, large paper mills produce PCC in a "composite" by recovering carbon dioxide, which is produced in the form of flue gases during combustion in power plants, by binding it to calcium hydroxide.

Natural calcium carbonate (limestone) is used in large quantities as a raw material for the building materials industry, as an aggregate in the steel industry, as a mineral fertilizer and as a mineral filler in various industrial applications such as paper, paints, varnishes, plasters, plastics and carpet backings. In total, more than five billion tons of limestone are mined every year. The main use is the production of cement (calcium silicate, calcium aluminate) and quicklime (Essabir, 2017)

Calcium carbonate is the most important filler by volume sold worldwide. Although more than five percent of the earth's crustconsists of calcium carbonate rocks, only a few deposits are suitable for the extraction of fillers, which should be as white as possible. The largest industrial user of white calcium carbonate is the paper industry with a quantity of over 10 million tons (worldwide) per year, followed by the plastics and building materials industry (plaster and paints) with a total of another 15 million tons per year. For use in the paper industry, especially as a coating color, deposits in Turkey, France, Italy, Germany, Norway and Austria are mined in Europe, with the mineral being crushed by wet grinding and sold as a slurry.

Calcium carbonate is approved as a food additive and food coloring and is often used when baking rolls, for example. For other applications, calcium carbonate is broken and/or ground and is sold in lumps or as flour. Natural calcium carbonates are not ideal for some applications, so synthetic calcium carbonates are used here (Erdogan, 2017), (Kremer, 2019).

1.5. ABS Plastic

ABS is the abbreviation for acrylonitrile butadiene styrene - for a plastic that is used under various trade names for a wide variety of products: for example as edge protection for furniture, as radiator grilles in cars or as housings for electronic devices. The substance enjoys particular attention and popularity as a starting material for workpieces in 3D printing. Acrylonitrile butadiene styrene is also a thermoplastic whose shape can be changed as often as desired at certain temperatures. The substance is solid and hard in a wide temperature range between -40 °C and +100 °C. Acrylonitrile butadiene styrene has a softening point of around 100 °C and liquefies between 220 °C and 250 °C. Acrylonitrile butadiene styrene was developed in the mid-20th century. Thermoplastic owes its global popularity to its versatility. It is moisture repellent, dirt repellent and highly resistant to fats and oils, electrostatic charging and temperature fluctuations. ABS is tough and hard, impact and scratch resistant.

Despite its strength, the fabric can be well prepared and processed into a finished product, for example by gluing and welding, grinding, drilling and sawing. Coating options also favor the use of ABS: it can be painted, printed and perfectly electroplated. It is very common to use ABS products with this metallic surface coating. It is precisely the high-quality galvanic surface coating that places ABS products in high demand worldwide. Metal-clad plastics are in great demand in electronics and the automotive supply industry. Surface metallized acrylonitrile butadiene styrene can be found as housing parts for small appliances such as smartphones, shavers and cameras. Housings for office machines, computers, TVs and vacuum cleaners are also often made from this thermoplastic. (Moore, 1973), (Peterson, 2019). ABS even entered the toy industry decades ago: LEGO building blocks are made from acrylonitrile butadiene styrene. Examples of ABS material are as follows; Wind instruments are made of ABS, in the furniture industry, medical products, electronic components, watch cases, sanitary fittings, helmets, sunglasses, etc. (Lauwaert, 2008).

ABS products in the automotive industry come in a wide variety of shapes and surface designs. This applies to body parts, spoilers, decorative strips or headlights, as well as various interior parts. The advantageous mechanical properties of acrylonitrile butadiene styrene copolymer can be further optimized in combination with other engineering plastics. A blend of the two thermoplastics ABS and PC (polycarbonate) results in a material that impresses with its added stiffness, low temperature impact strength, toughness and heat resistance. Such ABS/PC mixtures are used, for example, in production in the automotive sector and in the electrical and electronics industry. ABS blends are the materials from which things like the glove box, center console and belt guide slots are made. Mixtures are also used as standard for plugs, sockets, terminal blocks, cable ducts and electricity meters. These polymer blends are preferred, especially where the product is subjected to special mechanical loads. In addition to the excellent material properties, the attractive surface finish also impresses. The advent of 3D printing technology has increased awareness of acrylonitrile butadiene styrene worldwide. The quality characteristics of ABS filaments are specially selected. Acrylonitrile butadiene styrene (filament, fiber, yarn, usually wound on rolls or reels of different thicknesses) is a classic among 3D printer materials. The shapes created with ABS filaments impress with their high degree of hardness and smooth surfaces. They are durable and heat resistant (Peterson, 2019).

2. LITERATURE REVIEW

In the literature, there are studies in which thermo-plastic filaments and sandwich panel core material are produced using 3D printer and design form comparisons are made. Sugiyama et al. (2018) have produced sandwich panel cores in honeycomb, rhombus, rectangle and circle geometry using a continuous 3D carbon fiber printer (3D printer in which continuous and uncut fiber reinforcement is made on the thermoplastic melted in the extruder in the 3D printing process). As a result of their studies, they have seen that the strength of the core structure in equilateral geometry is the highest. Wang et al. (2017) examined the studies on the production of composite parts with various 3D printing technologies (FDM, SLS, SLA, etc.). They presented a critical perspective on the strength and material properties of composite parts produced with these technologies. As a result of their review, they reported that 3D printing technologies are low cost, high precision and flexible, so it is a convenient and preferable technology. Kabir et al. (2020) examined studies on the production of fiber reinforced composites with continuous 3D printing. They reported that fiber reinforcement material significantly increases the strength and mechanical properties of composite parts, 3D printing technology has a very wide usage area and has an important place among production methods. Quan et al. (2015) examined studies on additive manufacturing methods. They compared the strengths and weaknesses of 3D printing methods. As a result of their research, they determined that additive manufacturing technologies are a low-cost, versatile production method that provides high precision. Therefore, they reported that it is a preferable method in the production of reinforced composites. Sang et al. (2019) produced polylactic acid (PLA), basalt fiber reinforced PLA, polycaprolactone (PCL) filaments and produced cores in cylindrical, equilateral and honeycomb geometry by 3D printer using these filaments. As a result of the strength tests applied to these parts, they reported that the cylindrical geometry part produced from PLA-PCL30/KBF filament has a high energy absorption feature. Araya-Calvo et al. (2018) produced test samples with 3D printing technology using carbon fiber reinforced filament and investigated the effect of additive ratio on strength. They reported that the carbon fiber reinforcement provided the maximum compressive strength at a volume ratio of 24.44% and the maximum bending strength at a volume ratio of 48.93%. Çava (2019) produced standard test samples from ABS, PLA, HIPS and PETG filaments with a 3D printer and performed tensile, compression, 3-point bending and impact tests. It was determined that

PLA filament showed higher strength than other filaments. Then, he produced sandwich panel cores in different geometries (honeycomb and re-entrant), different cell-wall thickness and length with a 3D printer. It has been determined that the balpetic geometry provides the highest compressive strength, for both geometries, the compressive and bending values increase as the cell-wall thickness increases, and the compressive and flexural strengths decrease as the cell-wall length increases. In addition, composite (carbon epoxy prepreg) outer panels and sandwich panels were produced using structural adhesive and their strength properties were examined. Young et al. (2018) produced fracture test specimens using carbon fiber reinforced ABS filament with 3D printing technology and performed a Mode 1 loaded fracture test. As a result of the tests, it was determined that the parts produced with short fiber reinforced ABS decreased the fracture toughness.

In addition, certain ratios of carbon-fiber, natural fibers, etc. to the thermo-plastic filaments used in the literature. It has also been observed that strengthening works have been carried out by adding reinforcement materials. Yao et al. (2018) examined the literature on thermoplastic filament materials with carbon fiber added in depth. In the studies, they have seen that the carbon fiber additive significantly increases the mechanical and thermal properties. In addition, there are studies in which nanoparticle reinforced Composite plates are produced and tested. Some studies on the mechanical properties of composites are summarized below. Wetzel et al. (2003) used nano-sized Al_2O_3 (Alimuna) and $CaSiO_3$ (Calcium Silicate) additives to the polymer. The effects of additives in different mixing ratios on the flexural stiffness, flexural strength and fracture strength of the composite were investigated. Shuiping et al. (2017) produced polymers by adding silica nanoparticles to epoxy. They found that 3% silica additive increased the tensile strength of the polymer by approximately 61.9% and the impact strength by 55.5%. Zapata et al. (2019) added 3-5% $CaCO_3$ to low density polyethylene. As a result of their mechanical tests, they determined that the additive material increased the mechanical properties of the polymer by approximately 29%. Wetzel et al. (2006) added TiO and Al_2O_3 reinforcement to the epoxy. They performed 3-point bending test, dynamic mechanical analysis and compact fracture test on the doped epoxy polymer they produced. They observed that both additives increased the flexural stiffness, flexural strength and fracture strength of the polymer.

Bulut (2017) applied impact, bending and tensile tests to the graphene reinforced basalt/epoxy composite. It was determined that the flexural strength of graphene added to the epoxy at a rate of 0.1% increased by 28 MPa and the flexural modulus was increased by 2.81 GPa. Cristy et al. (2017) produced nanocomposites by adding 0-1-2-3% SiO_2 reinforcement to epoxy. Tensile and impact tests were applied to these nanocomposites. As a result, they found that 3% reinforcement increased the strength the most. Tuncer (2018) added $CaCO_3$, SiO_2 and graphene reinforcement materials to the epoxy and homogenized it with an ultrasonic mixer. Using these homogeneous epoxies, nanocomposites were produced by hand lay-up method and strength tests were applied. It has been determined that 1% SiO_2 additive increases the breaking strength by 7.57%, 3% $CaCO_3$ additive increases the breaking strength by 9.69% and 0.1% additive increases the breaking strength by 20%. Kim and Ye (2004) applied the Mode-I fracture test of carbon fiber/polyetherimide (PEI) composite at temperatures of 25-80-130°C. As a result of the fracture tests, it was determined that the energy absorbing ability and ductility of the material was the highest at 130 °C. Sales et al. (2017) produced CF / RTM-6 (resin transfer molding-6) by the VARTM (vacuum injection) method. Mod-I and Mod-II loaded fracture tests were applied to the composite at temperatures of 20°C and 80°C. They found that the fracture strength at 80°C was higher than at room temperature. Composite and sandwich panels have a wide range of uses and are widely used in important sectors of industry such as automotive, aerospace and construction. In addition, composite structures used in such a wide area are exposed to loads at different angles at the same rate. Therefore, it is very important to test these composite structures at different angles of loading. Fracture strength properties at different angles are determined by the mixed mode loading fracture test. Choupani (2008) investigated the mixed mode interlaminar fracture behavior of woven carbon fiber / polyetherimide (CF / PEI) thermoplastic composite material based on experimental and numerical analysis. Their experiments experimentally obtained mode-I, mode-II and a wide variety of mixed-mode data by varying the loading angle from 0° to 90° on modified Arcan specimens using special test apparatus. Using the finite element results, correction factors were applied to the CF/PEI fracture sample. The fracture surfaces of the CF/PEI composite under different mixed-mode loading conditions were examined by optical and scanning electron microscopy.

The features of composite sandwich structures, which are used extensively in the modern industry, are as follows; high hardness, high lightness, high strength, porous structure.

Composite sandwich panels have enormous advantages (light weight, longevity, impact strength) over standard plates.

Xie et al. (2020) investigated nomex honeycomb sandwich panels to provide sufficient data and theoretical support for the practical application. Therefore, it has become an indispensable structure in areas requiring high strength such as aircraft, ships, and space shuttles. Sandwich structures are divided into 3 basic types. The said varieties are: core structure foam, corrugated and honeycomb, etc. those of geometries. There are many studies on sandwich panels with corrugated core structure in the literature (Hou, 2013). St-Pierre et al. (2015) showed that corrugated sandwich panels exposed to dynamic loads show high strength in their studies. In addition, when they examined the bending properties, they found that the strength showed bending strength. In addition to these experimental studies, they provided a deep perspective to scientists on the effects of core structures on strength by making numerical modeling (finite element analysis). Again, in other studies in the literature, foam material was first placed between the steel panels and examined (L.L.Yan, 2014), (B.Han, 2015), (L.L. Yan, 2013). It was then experimentally compared with sandwich panels with cores of various geometries (B. Han, 2016). The results of the investigations show that the added nanocomposite structures increase the strength, stiffness and impact resistance of the corrugated sandwich panels. Bai et al. (2019) observed that the change in the properties of the core material has a great effect when different types of foam sandwich panels are impacted at low and high speed. They developed a method to detect the nonlinear response of laminates under loads. (R. Bai et al., 2019), (E. Tang et al., 2019), (Wang et al., 2013). Zhang et al. (2015) carried out various experimental studies on various geometries of honeycomb core structures. When they observed the effects of this honeycomb structure to change, they discovered that it provides high resistance. They found that the core structure of sandwich panels, when developed as honeycomb, has much higher strength than other (corrugated and foam core) structures. Wu et al. (2017) fabricated and tested metal honeycomb sandwich panels to study dynamic post-collision material properties and failure mode. A method based on the energy balance model was developed to compare the impact resistance properties of corrugated (honeycomb) core sandwich panels and standard panels (Yahaya, 2015). As a result of the comparisons, it was determined that the honeycomb structure showed the advantage of lightness and high strength. Sun et al. (2017) performed various tests (3 point bending, four point bending) on corrugated sandwich panels with honeycomb core. The results of their applications show that the numerical modeling they developed and the experimental studies overlapped with each other. They revealed that theoretical applications can be used easily to observe the effects of mechanical loads on sandwich panels (Crupi, 2007), (Belouettar, 2009). Hüseyin et al. (2019) investigated the collapse and bending properties of wood and concrete sandwich structures under loads. They revealed that the wood-concrete materials in the structures greatly affect and improve the strength properties of the sandwich panels (Hegarty, 2019). Many studies in the literature have revealed that composite sandwich panels, which are used in every field in modern industry, are becoming more widespread and expanding their usage area day by day (Xu et al., 2018), (Xu et al., 2019). Foo et al. (2007) developed a numerical model to detect the effect of core geometry on sandwich panels made of phenolic aramid papers. They found that the numerical results and the experimental results confirmed each other (S.Heimbs, 2009), (Roy 2014). In addition, sandwich panels with nomex core structure were investigated in depth under low and high strain rates in studies (Heimbs, 2007), (S. Xie et al. 2007), (Liu, 2015). Zhou et al. (2018) studied the effects of phenolic resins used in the production of nomex honeycombs on strength. They determined that the applied phenolic resin thickness had a direct effect on the strength. Rajanees et al. (2018) measured the mechanical properties of nomex honeycomb sandwich panels by compression and bending tests. İn addition, by developing a numerical (finite element) model, they were able to accurately determine the mechanical strength properties (Wu, 2019). Audibert et al. (2019) have produced sandwich panels with fiver reinforced cladding. The test specimens were examined by subjecting them to impact and shear loads. They were able to go beyond the theoretical framework with the compression/shear coupling model they developed. In experimental studies, sandwich panels with honeycomb core carry bending moment when subjected to mechanical loads. However, sandwich panels, which are exposed to a wide variety of loads in sectoral applications, cannot be tested experimentally. Innovative studies can be carried out by further developing the numerical analysis method developed in this thesis. (Park 2014). Using the model in this thesis, the sandwich panel can be tested in various geometric options by exposing it to various thermal or mechanical loads. According to the results of this study, the sandwich panel can be optimized.

3. MATERIALS AND METHODS

First of all, filament was produced using pure ABS granules. After this process, 1%, 2%, 3%, 5% $CaCO_3$ nanoparticle additive material was mixed into the pure ABS granule. Doped filaments were produced with granule mixtures with this additive added. Then, sandwich panel cores were produced with pure ABS filament and ABS filaments with $CaCO_3$ nanoparticle addition with a 3D printer. In order to investigate the effects of these additives on strength, 3-point bending tests and compression tests were carried out experimentally. Then, tensile tests were carried out in order to learn the material properties. 3-point bending and compression tests were simulated. Finite element analysis was performed using material properties learned from tensile tests. Experimental and finite element analysis results were compared.

3.1. Production of core material and sandwich panel test specimen

3.1.1. Filament production processes

The first step in the filament production process is plastic production. During refining, crude oil is heated in an industrial furnace that separates its many different components. One of the components, naphtha (A product between gasoline and kerosene, obtained from the distillation of petroleum between 100 ^oC and 250 ^oC), is most often used in the manufacture of plastics for 3D printing. Naphtha, catalysts and other chemical components are chemically bonded in the polymerization reactor. The polymerized naphtha products are then combined and processed. This process involves melting the products and youmixing them with other materials to form the plastic. The resulting plastic is then granulated into small pieces known as pellets or resin. Plastic suppliers typically produce clear or white granules and resins. This allows their users, such as material manufacturers, to have more control over the dyeing process. When compared to ready-to-use filaments and granules, granules are much cheaper in cost. In the second step of the process, the granules are prepared for the next step, forming, where they harden into a filamentous shape. The granules are placed in an industrial mixer and mixed with additives to create a homogeneous mixture and impart special properties to the material. Additives may contain colorants or other elements that affect properties such as impact resistance, strength, structural integrity, and even magnetic properties. After the granules are properly mixed, the drying stage is started. Like the filament, the granules are hygroscopic. This means that they absorb moisture from the air. This can deform or break the plastic, so it is very important to remove moisture from the pellets to ensure quality filament production. Drying is usually carried out at 60°C to 80°C for several hours, but the process depends on the manufacturer. The third step in the 3D printer filament manufacturing process is to shape the granules into arrays. This step includes the heating and cooling process. This is one of the most important and responsible steps. In the first molding step, the pellets are fed into a material extruder containing a heating chamber. In this chamber, the individual granules are melted into a sticky substance so that they can be easily shaped. In this case, the granules are combined and form a continuously spun material. The bonded thread material, better known as filament, exits the heating chamber through a round nozzle and enters the cooling section. After leaving the filament heating section, it passes through several water chambers. The first chamber is filled with warm water, which is an important factor in obtaining a round thread. Correctly setting the temperature depending on the material helps avoid oval shaped filament which can cause problems for 3D printing. The second chamber is filled with cold water or air, which cools and reshapes the yarn. The speed at which the thread is pulled determines the diameter of the thread. A lower speed produces a larger diameter and a higher speed does the opposite. During this step in the production of the 3D printable material, motors pull the filament from the cooling chamber to the winding mechanism. The winding process begins with measuring the filament diameter with a laser device to make sure it is within the tolerance of the final required diameter, most likely 1.75 mm or 2.85 mm. The yarn is then tied to a spool and wrapped around it. As soon as the sensors detect that the spool is full, the thread is cut and fixed. The process starts again, filling the next spool until the filament lot is finished. Figure 3.1. shows the filament production machine in the university's laboratory.

Figure 3.1. Filament production machine in our laboratory

3.1.2. Production of $CaCO_3$ added ABS filament

In this study, the filament production machine in our laboratory was used for the production of reinforced filament. In order to produce doped filament in the filament production machine, Pure ABS granules and reinforcement nano-particles ($CaCO_3$) are mixed and thrown into the chamber where the cutter is located. The materials thrown into the hopper are shredded with stainless blades. The shredded materials are transferred to the extruder section, where they will be melted homogeneously by temperature. ABS / nanoparticle added materials are melted from the nozzle and pressed outward from the extruder tip. After this process, it is cooled and rolled up, so that it becomes the final product to be used as a printing material in the 3D printer.

Filaments were produced using pure ABS granules and granule mixtures with $CaCO_3$ additive added. The additive ratios in doped filaments are as follows;

- %100 ABS
- %99 ABS+ %1 $CaCO_3$
- %98 ABS+ %2 $CaCO_3$
- %97 ABS+ %3 $CaCO_3$
- %95 ABS+ %5 $CaCO_3$

3.1.3. Sandwich panel core production with 3D printer

The list of 3D printing technologies and processes is constantly growing, as 3D printing is constantly changing. The 3D printing industry continues to improve its hardware, as well as the materials and processes used to create objects or parts. It is important to choose the right

3D printing process and the right material, depending on many factors such as budget, design or function. 3D printing can create many different 3D printed objects that were previously only mass-produced. In FDM, molten plastic is applied to a work platform. As with any 3D printing process, the key requirement here is a printable, digital 3D model. This model is split (sliced) into multiple layers by a computer program. These layers are then applied to a working level by an extruder. The extruder is a heatable nozzle. The plastic threads (called filaments) used for printing are heated by the extruder until they liquefy. This liquid thermoplastic is applied to the working plane by the extruder according to the layers of the 3D model. The material hardens rapidly after cooling. The next layer of liquid plastic is applied to a hardened layer. This creates the actual image of the 3D model layer by layer. In this process, solid bodies are printed with padding structures ('padding'), not solids. Support structures for overhanging elements must also be printed. This process is similar to using a hot glue gun, where glue sticks are heated from the nozzle and applied to the workpiece to be bonded. The FDM process (compared to the 3D printing process) is very inexpensive and relatively quick to print. As a result, early prototypes can be created, tested and corrected with almost no problems. Due to the high inaccuracy of the process, other processes are preferable for advanced prototypes or small series (e. g. laser sintering, stereolithography, polyjet). ABS is a popular plastic for model making. The good surface hardness and impact resistance as well as a wide range of processing options make ABS a well-suited material for functional models and models that are to be preferred. By using the undoped (Figure 3.2.) and doped filaments produced in the previous stage of this study as 3D printer printing raw material, 3 point bending test cores and compression test cores were produced. The 3D printer heats and melts these filaments in the extruder chamber, making layer-by-layer printing and producing test samples.

Figure 3.2. Pure ABS filament

With the SOLIDWORKS program, sandwich panel core test specimen designs with honeycomb geometry in accordance with ASTM Standards (ASTM C365 ASTM C364, ASTM C393) were transferred to the FLASHFORGE 3D printer program (Figure 3.3.) in STL (Standard Triangle Language) format.

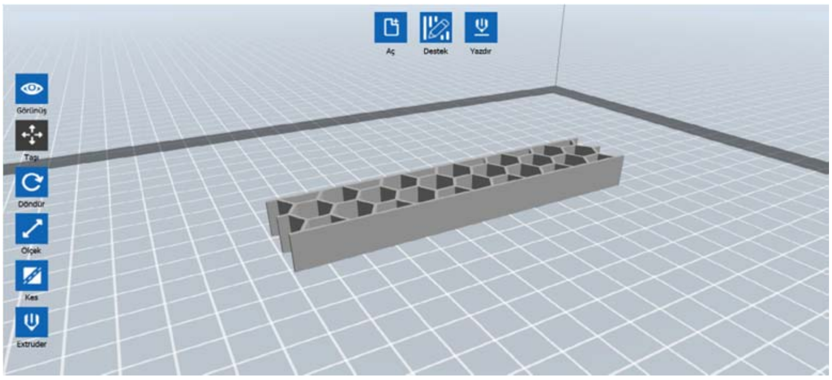

Figure 3.3. 3D printer's software

The printing parameters of the 3D printer standardized so that the comparison is objective. Printer parameters standards given in Table 3.1.

Table 3.1. 3D printer printing parameters

Layer thickness	0.18 mm
Solidity ratio	%100
Form of Occupancy	Honeycomb
Print Speed	60 mm/sn
Browsing Speed	80 mm/sn
Heat	230℃
Table Temperature	120℃

In addition, tensile test samples were printed using $CaCO_3$ added ABS filament (Figure 3.4.). The results from the tensile test samples will be used in the finite element analysis to be done in ANSYS.

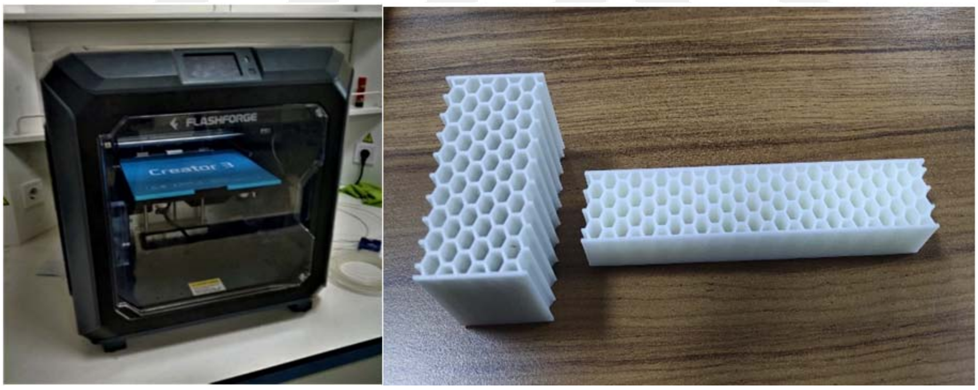

Figure 3.4. 3D printer and 3D printed honeycomb core

Figure 3.5. Tensile-compression testing machine

The tensile test was applied to these test samples with the tensile device (Figure 3.5) in our laboratory.

3.1.4. Production of Composite plates (Sandwich panel outer surfaces) and composite test specimens

The outer surface plates of the sandwich panels are produced by vacuum infusion method using carbon fiber fabric and epoxy. The vacuum infusion method is a method that combines fiber cloth and resin with vacuum pressure. In this method, which is made by penetration of the resin into the vacuumed environment, glass fiber reinforcements are placed on the glass, infusion bags are placed on these reinforcements in order to provide sealing, and the resin is applied to the mold with the help of vacuum. Composite plates produced by vacuum infusion method are shown in Figure 3.6.

Figure 3.6. Composite plate production by vacuum infusion method

When the epoxy fiber penetrates the fabric, the additives take their place among the fiber fibers. Thus, Composite plate is produced.

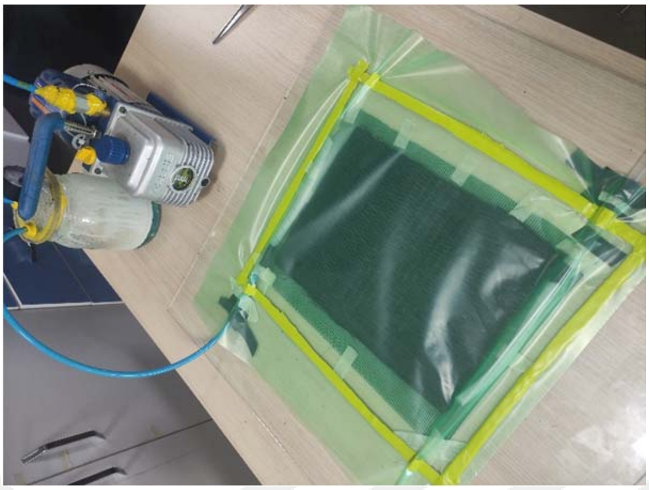

Figure 3.7. Composite plate production by vacuum infusion method

After these processes, the Composite plates were finalized with water jet Figure 3.7. shows the Composite plate cut with water jet.

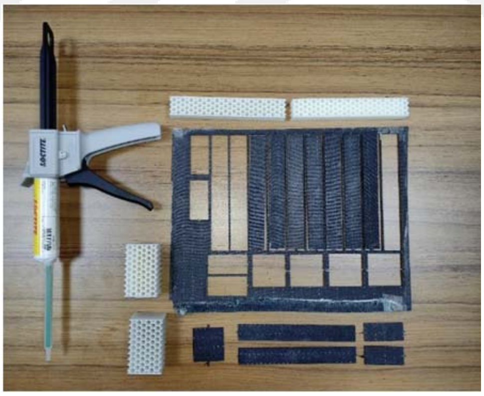

Figure 3.8. Structural adhesive, core structures and waterjet cut composite plates

Composite sandwich panel samples were produced by combining structural adhesive and core materials. Composite plate bonding process is shown in Figure 3.9.

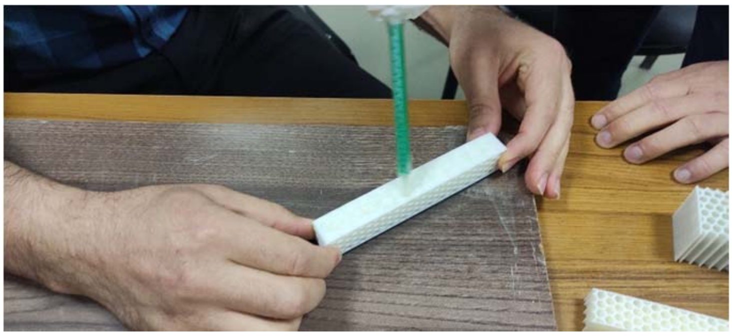

Figure 3.9. Composite plate bonding process

Composite sandwich test specimens after bonding are shown in Figure 3.10.

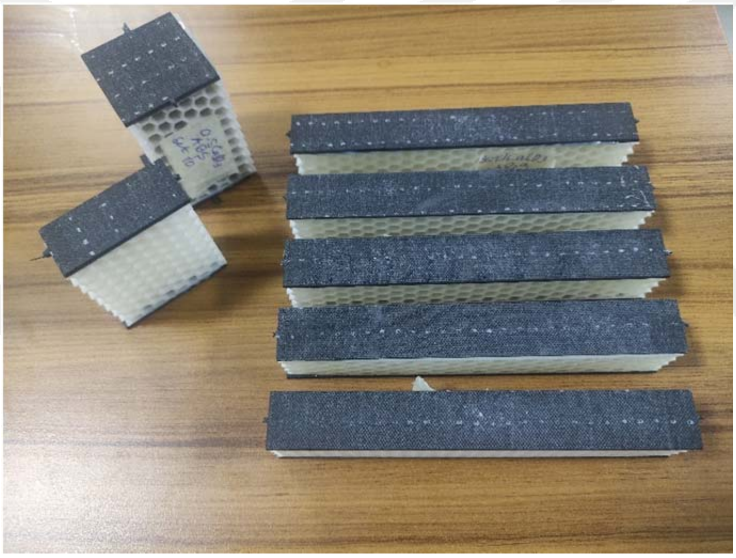

Figure 3.10. Composite sandwich panel test specimens

3.2. Application of tests

3.2.1. 3 Point Bending Test

In the 3-point bending test, a standardized sample of material is bent until plastic deformation begins or breaks. In the 3-point bending test, a sample is subjected to uniaxial bending stress (tensile and compression) to obtain information about the bending behavior of materials. Sandwich panels are tested in flexural tests and flexural strength, deflection at break and modulus of elasticity are determined. To perform the test, a standardized specimen is placed on two support rollers (line contact) of a bending testing machine and bent with a printing plate in the middle of a stamping stamp with increasing force. Because of the three pressure points (two side cylinders and middle cylinder), this test arrangement is called a 3-point bending test. The bending test is a test performed by pressing the center of a circular or rectangular test apparatus on a piece that is placed freely on two supports in a vertical position. It allows the determination of plastic deformation and strength values of the test sample. The bending stress is greatest in the section with maximum deflection, that is, in the middle of the sample. This is where the greatest torque always reigns. In the case of bending, this torque is also called bending moment. Starting from the center of the specimen, the bending moment decreases linearly up to the two support bearings. The 3-point bending test (Figure 3.11.) is applied to determine the design information about the strength of the material. It is done to determine the mechanical properties of the material against bending. Bending strength occurs in every region of the material due to bending stress. Since the material is homogeneous and obeys Hooke's laws, calculations can be made with standard bending formulations. The 3-point bending test is the deformation that occurs when a force is applied in the middle of a flat test piece of circular or rectangular cross-section, which is placed on the free support, without changing direction. The values to be calculated as a result of the 3-point bending test are as follows; bending moment , bending stress , modulus of elasticity , amount of deflection.

Figure 3.11. 3-point bending test

When a force is applied to the specimen of the 3-point bending test, a compressive stress occurs in one part of the specimen section and a tensile stress in the rest of the section.

The application of the 3-point bending test is mainly based on the "simple beam" model. Since the beam equation is derived according to the ideal moment state, it is desired that the shear stress in the beam remains at a negligible level compared to the normal stresses. While the test is being applied, the deflection value formed in the middle of the sample is measured while the F force is increased. As a result of the 3-point bending test, the deflection corresponding to the applied force is measured. Measurements are made according to the highest bending and deflection point, which is the midpoint of the part (Fig. 3.12), (He, 2008).

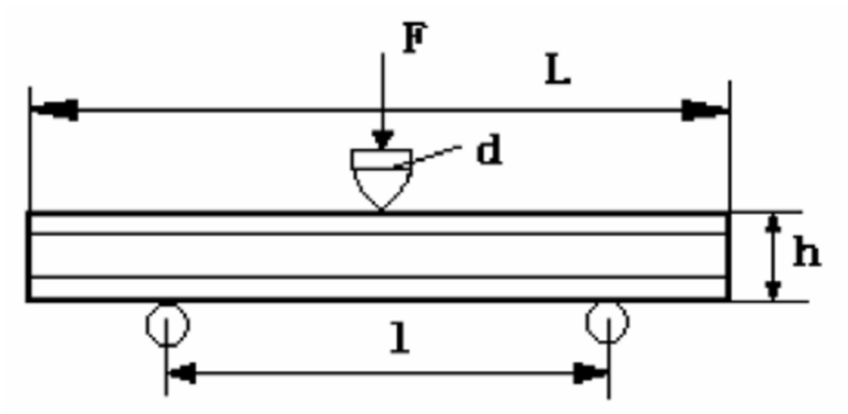

Figure 3.12. Shematic diagram of 3-point bending test

If the 3-point bending test is a homogeneous and elastic beam, the maximum stress occurs at the midpoint on the outer surface of the beam. This stress on the outer surface is calculated for any point of the load deflection curve with the following formula. The 3 point bending test sample is shown in the Figure 3.13.

$$\sigma_e = 3Pl/2bh^2 \quad (4)$$

where σ_e represents the stress on beam surface at midpoint (N/mm^2) (Maximum Bending Stress), P is the force (N) at any point of the load deflection curve, l is the distance between two supports (mm), b is the beam width (mm) and h is the height of beam (mm).

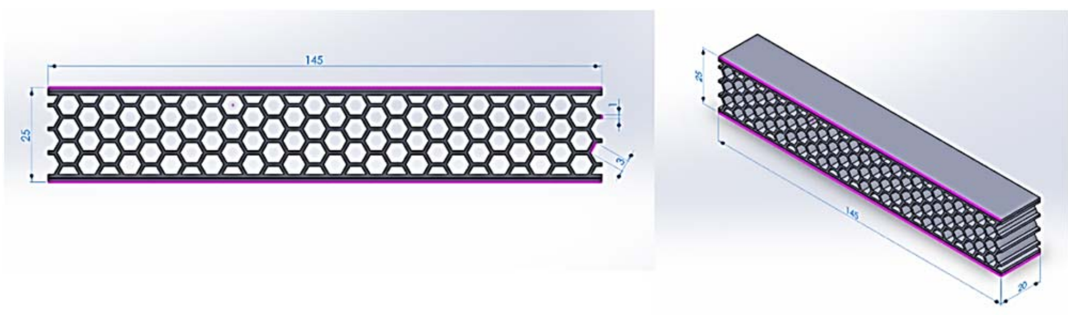

Figure 3.13. 3-point bending test specimens

3.2.2. Compression Test

The sandwich panel is lightly compressed at both ends of the test device and subjected to a compression force parallel to the plane of the panel. This method, called compression testing, is shown in the Figure 3.14. The force is mainly applied at the ends of the cover plates, some of the force is transmitted to the cover plates by friction in the end clamps. Strength is defined by dividing the applied force by the total cross-sectional area of the two faces. Acceptable failure modes are those that occur away from the clamped ends. A typical malfunction is the formation of wrinkles or dents on the cover pages. It is the test made by exposing the part to compression forces. It is used to determine the resistance and behavior of the part under the effect of compression force.

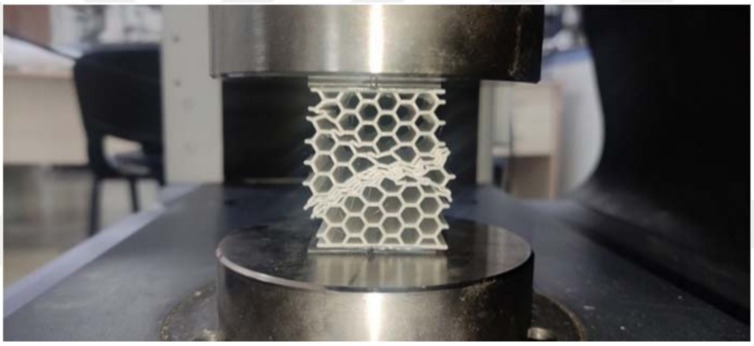

Figure 3.14. Compression test

Compression test is performed to determine the mechanical properties of metallic and non-metallic materials such as compression yield strength, compressive strength, compressive elasticity modulus, deformation, % change in section, under static loading conditions.
The compression test is the opposite of the tensile test in terms of the application of the load and its effects on the specimen. Compression test is also done in universal devices and a pressure load increasing with constant speed is applied to the sample placed between two compression heads. As a result of this compression load, while the sample length is constantly shortening, the cross-sectional area of the sample is constantly increasing. Compressive stress is the resistance of the material to compression. The stress value is found by dividing the force by the cross-sectional area. The maximum resistance of a material to compression is found by compression test. In the compression test, the object shortens for a while, then either breaks or

crushes, or retains its shape if sufficient force is not given. The dimensions of the test sample produced for use in this test study are shown in the Figure 3.15.

$$\sigma_b = P_I / A_0 \qquad (5)$$

where σ_b represents the compressive stress, P_I is the head load and A_0 is the original cross-sectional area of the sample.

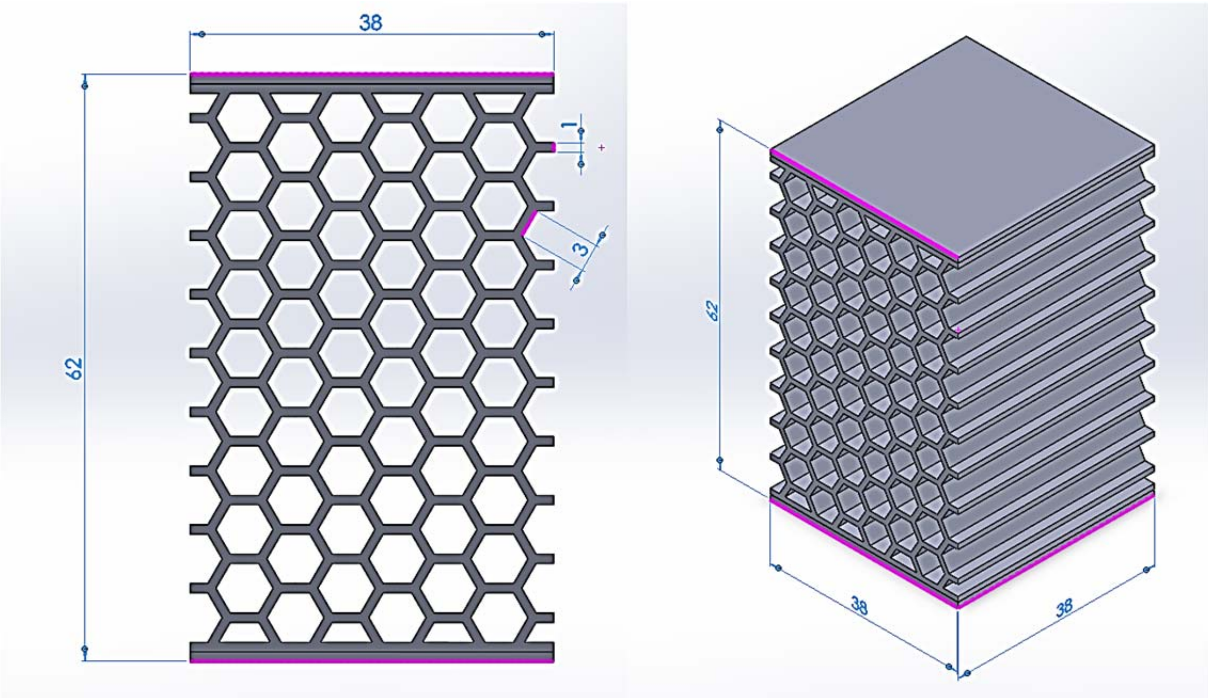

Figure 3.15. Compression test specimens

3.2.3. Tensile Testing

Tensile testing is a standardized procedure in materials testing. It can be used to determine tensile strength, elongation at break and yield point as well as other material parameters. Tensile testing is one of the destructive, quasi-static testing methods as the material is loaded beyond its yield point. In a tensile test, standardized specimens with a defined cross-sectional area are stretched until they break. The measurement results from the tensile test are listed in the rated stress/total elongation diagram. From this, technical recyclable material parameters can be read. In the tensile test, the elasticity modulus is determined by the following material properties. Many materials behave in a linear-elastic fashion at the start of a force. This means that the deformation is completely reversible when the load is unloaded, as long as the yield point is not reached. The linear-elastic deformation behavior is defined by the material value of the modulus of elasticity E. The material value in this case corresponds to the slope of Hooke's straight line.

The tensile strength is one of the most important characteristic values of precious materials and represents the maximum of the tensile hardening curve. The elongation characteristic value of the tensile strength is uniform elongation: Up to this point, the samples in the tensile test do not show any macroscopic contraction. The section does not shrink, unlike materials that do not deteriorate after reaching tensile strength and then show a clearly recognizable necking.

Tensile test specimens were produced with pure ABS filament and doped ABS filaments produced with $CaCO_3$ additive at mixing ratios of 1%, 2%, 3%, 5%. Tensile test specimens with the same additive ratio produced were produced in X, Y and Z axes in order to determine orthotropic material properties. Then, it was exposed to tensile load with the tensile test device (Figure 3.16.) in our laboratory. In this way, orthotropic material properties of filaments with various additive ratios were determined. These material properties were used in the finite element analysis.

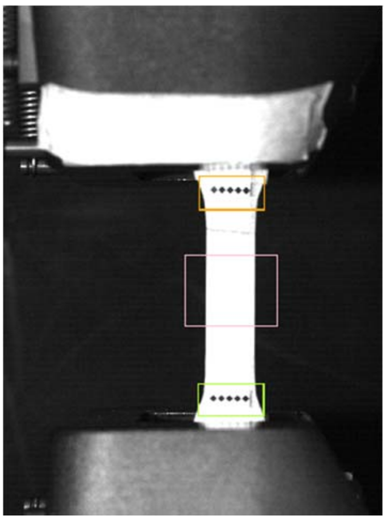

Figure 3.16. Tensile test

Tensile strength (σ_t) : It is defined as the highest tensile stress that a material can withstand until it breaks or breaks.

This stress is the highest stress value in the tensile diagram and is found by the formula below.

$$\sigma_t = P_I / A_0 \tag{5}$$

$$\varepsilon = \Delta L / L_0 \tag{6}$$

Where presents ε is unit strain and the ratio of the length change (ΔL) that occurs when the force is applied to the material, to the initial length (L_0) before the force is applied. Modulus of Elasticity (E) is a measure of the strength (strength) of the material. It is the result of the linear relationship between unit strain and normal stress (tensile or compressive stress) and is defined as stress per unit elongation. The linear relationship between strain and normal stress (tensile or compressive stress) can be defined as:

$$\varepsilon = \sigma_t / E \tag{7}$$

3.2.4. Finite Element Analysis

The finite element method (FEM) is a numerical method used in the context of simulations for targeted structural analysis and optimization. Finite element analysis (FEA) is a numerical method in which the area to be examined is divided into a finite number of elements. The overall behavior of the structure can be calculated from the behavior of individual subdomains using appropriate algorithms. The application areas of the method are diverse. A mechanical engineer uses an FE program to calculate whether a part, component, or system can withstand applied loads. In this thesis, it was used in numerical testing of strength tests applied on sandwich panels. With FEM, small areas of a component or a compute area are used to map the physical behavior of the component. Through this method, an object and its behavior are made computable under the influence of forces, heat or vibration. Individual items are defined by nodes. For each of these discrete elements, simple approximation functions that map physical behavior are selected and used. The physical behavior of the whole body is modeled by how these elements respond to forces, loads, and boundary conditions, and how charges and reactions propagate as they move from one element to another through very specific problem-dependent continuity conditions under which the approach functions. The FEM obtains an approximate solution of the differential equation by using the difference parts and evaluating them numerically. However, this procedure includes approaches. To use the method logically, the computational engineer must have knowledge of how his component is loaded and what effects can occur. A calculation based on the FEM is performed in three steps:

The model is prepared during preprocessing. With meshing (also meshing), the component surface is split into finite elements. Triangles and quadrilaterals, tetrahedrons, cuboids, and even Lagrangian elements exist. On the one hand, the thinness of the subdivision has a significant effect on the accuracy of the approximate calculation results; on the other hand, the computation time required increases with the density of the network. The material is then assigned because the behavior of the material to external loads is decisive for the mechanical strength analysis. Finally, boundary conditions such as loads are defined. The second step is to solve the equations. A software program for mathematical problems, called the solver, solves the system of equations behind a FEM model. Systems of equations with 10 million or more equations are not unthinkable and unsolvable. The first result includes displacements of individual nodes. Disturbances, stresses and knot forces can then be calculated. Solvents are available for mechanical, thermal, electrical or magnetic variables and combinations. The results are evaluated after the procedure. Graphical representation of result variables is common, often due to the large number of results originating from a large number of elements. Color charts are used for this, providing a quick overview of the results. In addition, additional results are often produced during post-processing. Equivalent stress is an example. 3D CAD files to be used in finite element analysis were designed with the SolidWorks (Figure 3.17.) program. The FEA was performed by transferring the files, which were output as ".step" file in the SolidWorks file, to the ANSYS program. The process using the ACP pre and Static Structural modules is explained step by step below.

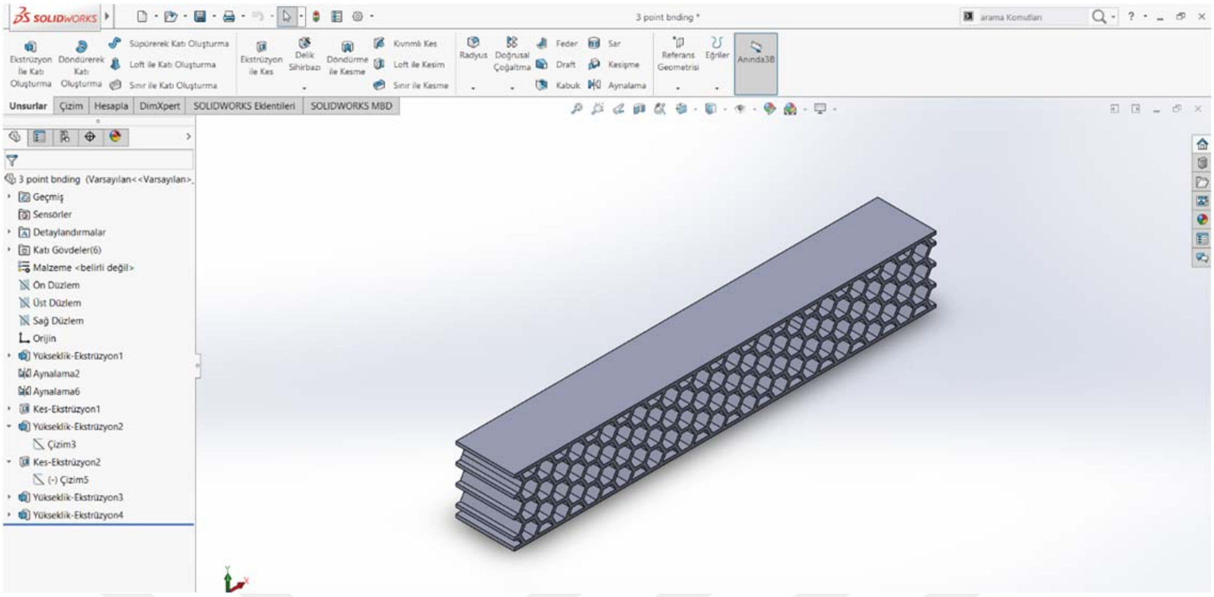

Figure 3.17. Core of 3-point bending test specimens designed with SolidWorks

The ".step" files designed in the first stage were transferred to the ACP Pre module of the ANSYS program. Figure 3.18. shows the ANSYS project file.

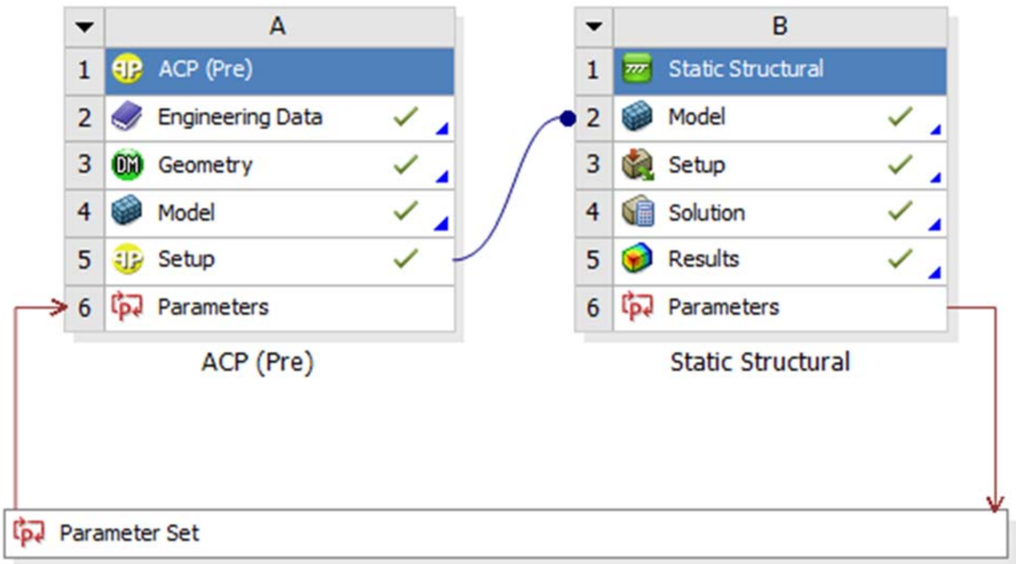

Figure 3.18. ANSYS project file image

3-layer carbon fiber plates (at 90/0/90 degree angles) were placed on the lower and upper parts of the sandwich panel core structures transferred to the ANSYS program by using the ACP Pre module. The image of the designed composite plates is given in Figure 3.19., Figure 3.20.

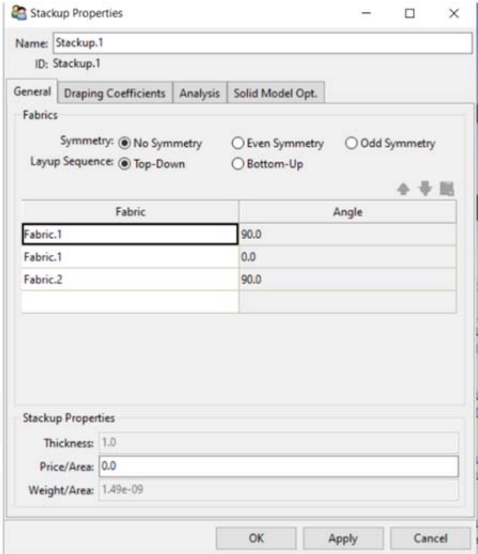

Figure 3.19. Carbon fiber panel design

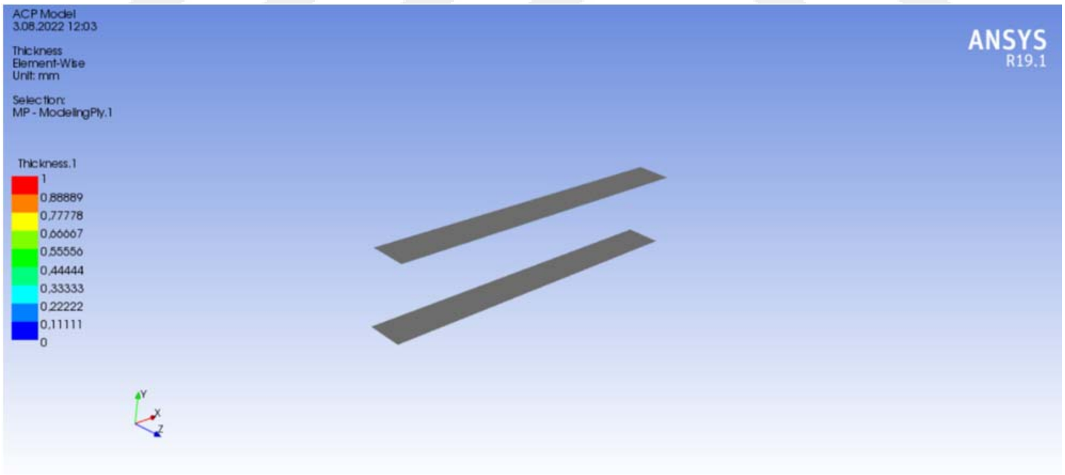

Figure 3.20. Bottom and top carbon fiber plates of the sandwich panel

The 3-point bending test is modeled exactly the same in ANSYS. Modeled 3-point bending test image is given in Figure 3.21.

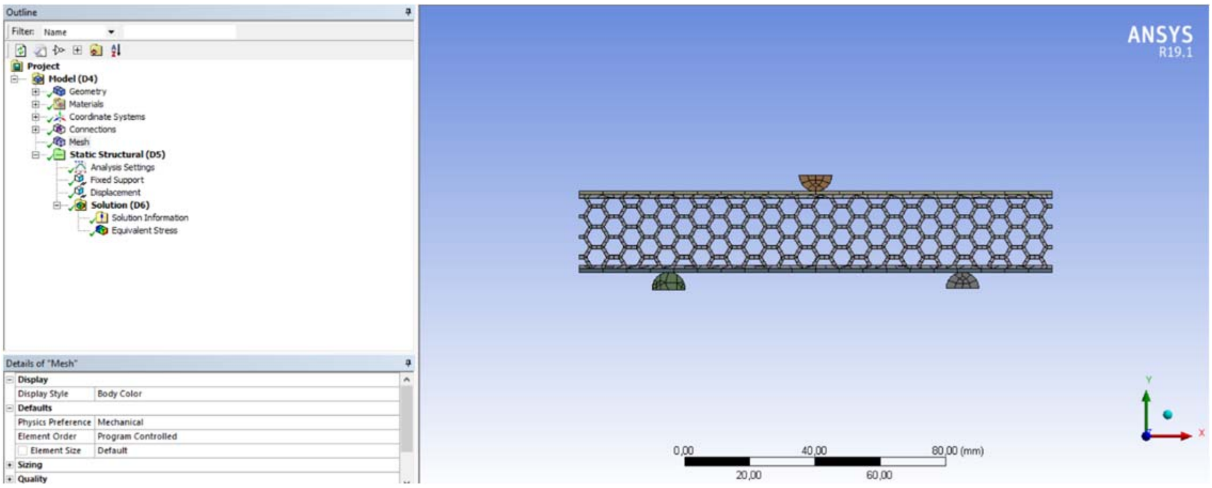

Figure 3.21. Bottom-top carbon fiber plates, honeycomb core structure and additional parts that apply samples of 3-point bending test

A quadratic or higher-order item uses a non-linear shape function. Displacements between nodes are interpolated using a higher order polynomial. These items have mid-side nodes. An element edge consists of three nodes instead of two. Quadratic elements are more suitable for representing complex geometries and bending deformations. In this thesis, the quadratic FE element type was chosen because complex structures were tested. Mesh selections are;

- Physics Preference: Mechanical
- Element Order: Quadratic
- Nodes: 22504
- Elements: 3315
- Minimum Edge Length: 1, mm
- Span Angle Center: Fine

Even when the values of these selections were amplified, the results were not much affected due to the relatively small structures of the test samples. In this context, the choices in this thesis study were sufficient to reach the right results. In the finite element analysis, the auxiliary cylinders on which the sample sits are fixed from their lower parts (Figure 3.22.).

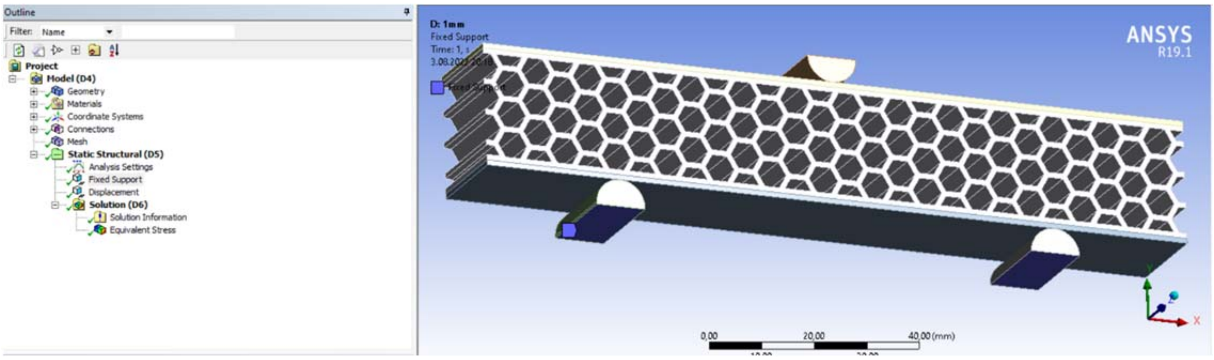

Figure 3.22. Bottom fixed half cylinders

Previously, applied 3-point bending tests were examined and as a result of these tests, it was determined that the part reached the maximum stress was 15 mm. Then, in order to simulate the 3-point bending test, the half-cylinder advance was given to the half cylinder at the top of the sample. In addition, as mentioned in the previous sections, the orthotropic material properties of the filaments with different additive ratios were determined by the tensile test. These orthotropic properties obtained were entered separately for each material to be tested and finite element analysis was performed.

Note: The same method was used in modeling the compression tests in the ANSYS program.

4. RESULTS AND DISCUSSIONS

4.1. 3-Point Bending Test Results

Test samples produced using 1%, 2%, 3%, 5% $CaCO_3$ added filaments and pure ABS filament were subjected to 3-point bending test. Figure 4.1. shows the sample that was subjected to the 3-point bending test.

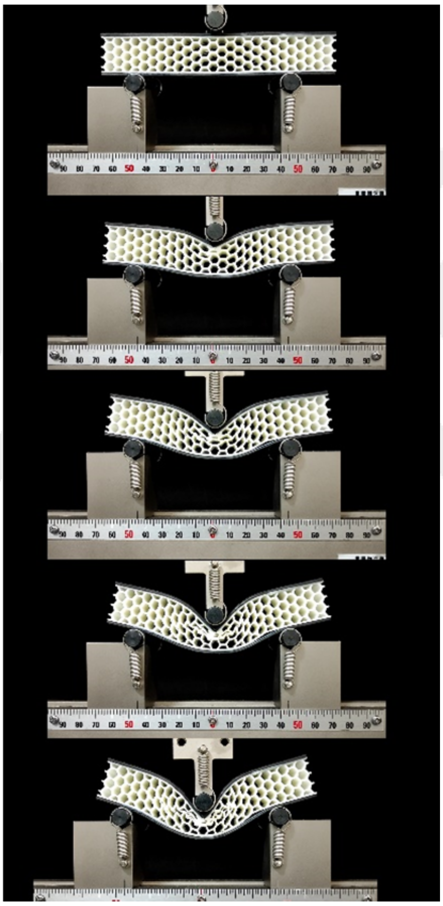

Figure 4.1. Three-point bending test step-by-step view

The 3 point bending test results (Figure 4.2.) are as follows;

- The test specimen produced with pure ABS filament withstands a load of 801.94 N,
- The test sample produced with ABS filament with 1% $CaCO_3$ nanoparticle additive resisted 1278.73 N load,
- The test sample produced with ABS filament with 2% $CaCO_3$ nanoparticle additive resisted 1382.33 N load,

- The test sample produced with ABS filament with 3% $CaCO_3$ nanoparticle additive resisted 1518.504 N load,
- The test sample produced with ABS filament with 5% $CaCO_3$ nanoparticle additive resisted

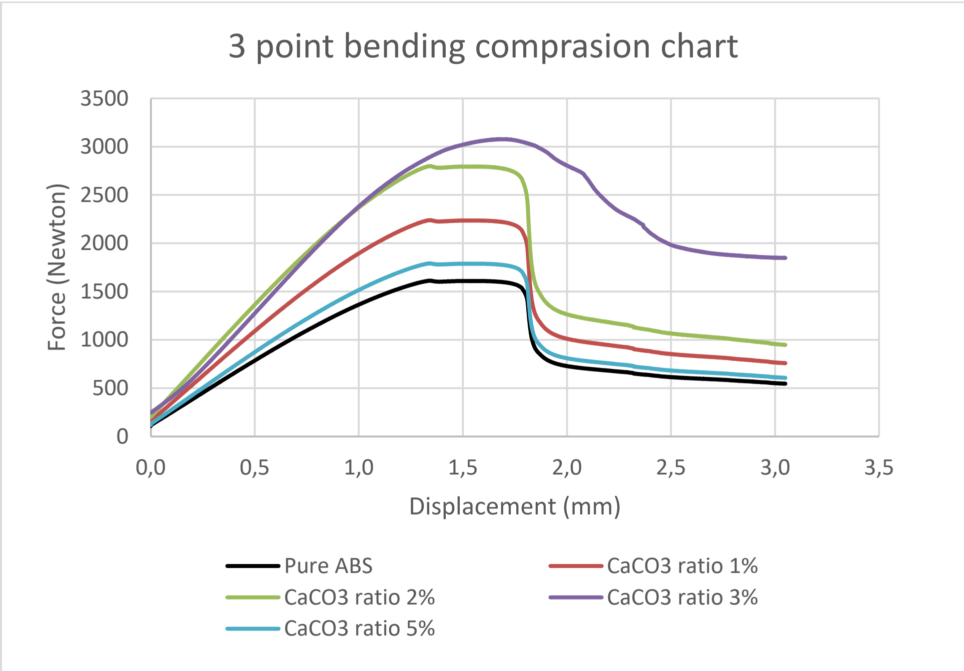

Figure 4.2. 3-point bending test comparison chart

4.2. Compression Test Results

The compression test is the opposite of the tensile test in terms of the application of the load and its effects on the specimen. Compression test is also done in universal devices and a pressure load increasing with constant speed is applied to the sample placed between two compression heads. As a result of this compression load, while the sample length is constantly shortening, the cross-sectional area of the sample is constantly increasing. In practice, the materials used where compressive forces are applied are generally brittle materials. The compressive strengths of metallic materials such as gray cast iron, bearing alloys and non-metallic materials such as brick and concrete differ from their tensile strength. Since it is much higher, such materials are used where compression forces are applied and are examined by compression test. At the end of the compression test, a compression load-shortening curve is drawn by the device. This curve is exactly the same as the load-strain curve obtained in the tensile test. However, the axes show the compression load and the shortening of the sample as a result of this load. Compression-strain curve is also not used directly in engineering calculations, but is converted to engineering compressive stress and engineering strain, as in the tensile test. Test samples produced using pure ABS filament and ABS filaments with 1%, 2%, 3%, 5% $CaCO_3$ additives were subjected to compression test. Figure 4.3. shows the sample that was subjected to the compression test.

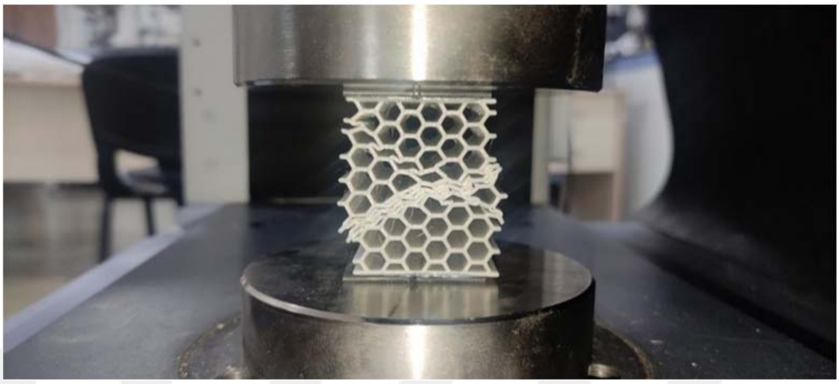

Figure 4.3. Sample with compression test

The compression test results (Figure 4.4.) are as follows; the test specimen produced with pure ABS filament withstands a load of 1611.77 N, the test sample produced with ABS filament with 1% $CaCO_3$ nanoparticle additive resisted to a load of 2238.57 N, the test sample produced with ABS filament with 2% $CaCO_3$ nanoparticle additive resisted 2798.21 N load, the test sample produced with ABS filament with 3% $CaCO_3$ nanoparticle additive resisted a load of 3077.28 N, the test sample produced with ABS filament with 5% $CaCO_3$ nanoparticle additive resisted a load of 1790.85 N.

As seen in Figure 4.4., the test sample with 3% $CaCO_3$ added showed the highest strength (3077.28 N).

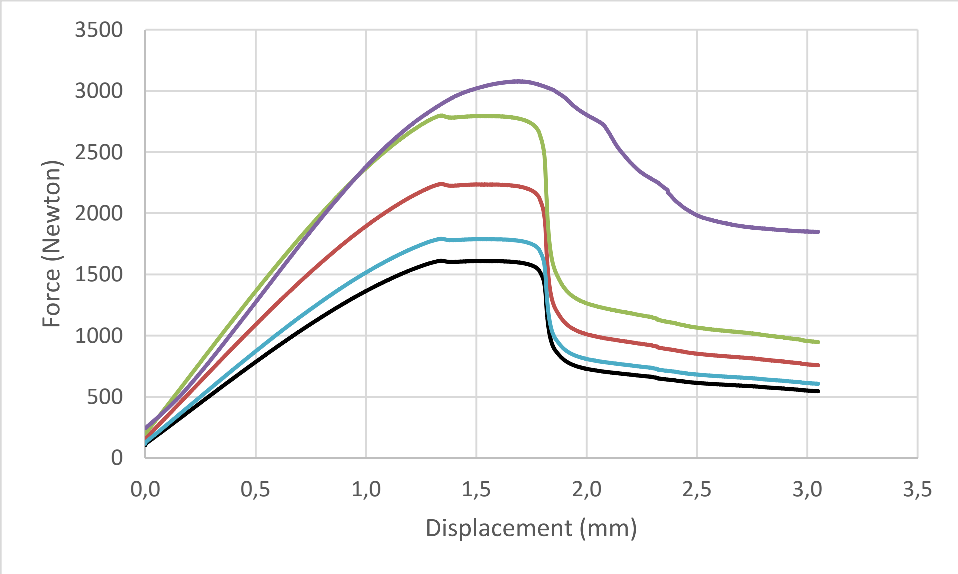

Figure 4.4. Compression test comparison chart

4.3. Finite Element Analysis 3-Point Bend Test and Compression Test Results

The material properties of the samples with different additive ratios, which were subjected to tensile testing, were determined. Orthogonally isotropic properties of ABS samples containing different ratios of $CaCO_3$ nanoparticles and printed at conditions of 100% filling ratio, 40mm/min printing speed, 0.15mm layer thickness and with triangular internal architecture are given in Table 4.1. This material has been added especially by assigning new material in the ANSYS program. In this way, results close to the application tests were obtained in the analyses performed in the ANSYS program.

Table 4.1. Orthotropic material properties

	E_1=E_2 (MPa)	ν_{12}=ν_{21}	σ_{y1}=σ_{y2} (MPa)	σ_{u1}=σ_{u2} (MPa)
Pure ABS	1737.4	0.341	24.8	31.24
	E_3 (MPa)	ν_{31}	σ_{y3} (MPa)	σ_{u3} (MPa)
	1637.9	0.298	21	26.7
1wt% $CaCO_3$	E_1=E_2 (MPa)	ν_{12}=ν_{21}	σ_{y1}=σ_{y2} (MPa)	σ_{u1}=σ_{u2} (MPa)
	1995.3	0.311	27	32.83
	E_3 (MPa)	ν_{31}	σ_{y3} (MPa)	σ_{u3} (MPa)
	1759.4	0.346	22.6	28.45
3wt% $CaCO_3$	E_1=E_2 (MPa)	ν_{12}=ν_{21}	σ_{y1}=σ_{y2} (MPa)	σ_{u1}=σ_{u2} (MPa)
	2123	0.321	28.3	35.34
	E_3 (MPa)	ν_{31}	σ_{y3} (MPa)	σ_{u3} (MPa)
	2033.4	0.324	28.3	32.26
5wt% $CaCO_3$	E_1=E_2 (MPa)	ν_{12}=ν_{21}	σ_{y1}=σ_{y2} (MPa)	σ_{u1}=σ_{u2} (MPa)
	1389	0.289	18.3	24.32
	E_3 (MPa)	ν_{31}	σ_{y3} (MPa)	σ_{u3} (MPa)
	1303.7	0.283	16.6	22.71

4.3.1. Finite Element Analysis 3-Point Bending Test Results

The test specimens were modeled numerically in the ANSYS program using the material properties obtained in the previous application tensile tests. In the modeled test samples, firstly, pure ABS material properties were used. Then, reinforced ABS plastic properties with 1%, 2%, 3%, 5% $CaCO_3$ additives were used for comparison in the numerical model. The finite element analysis results simulating the 3-point bending test with the Ansys program are given below. The 3-point bending test result of the sandwich panel modeled with pure ABS material properties is given in Figure 4.5. As a result of this analysis, this simulated test sample resisted a maximum loading of 17.799 MPa.

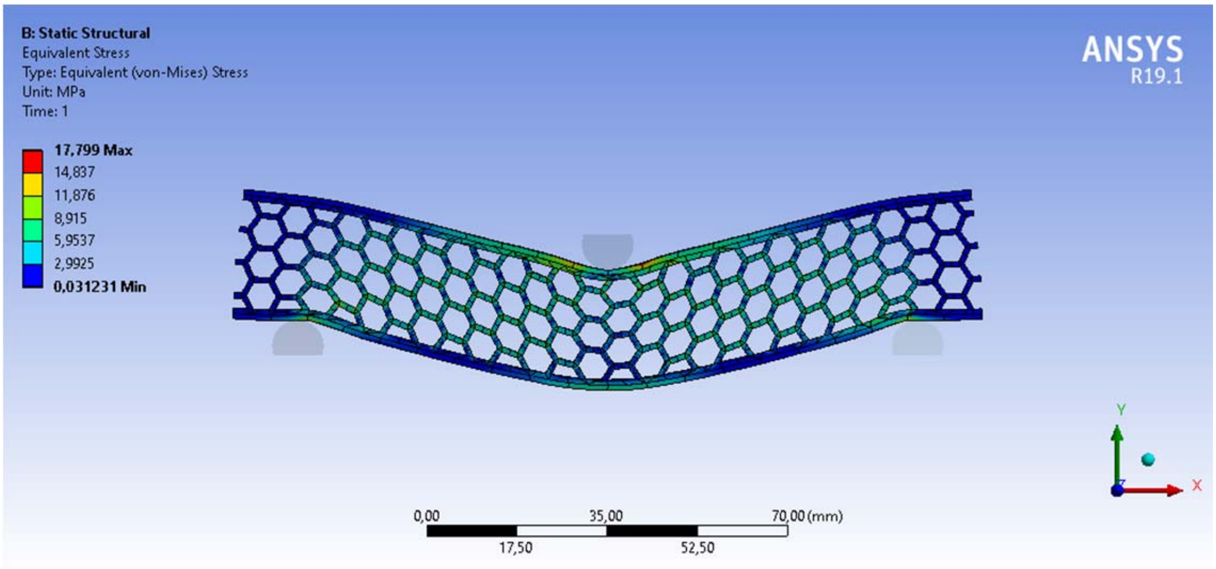

Figure 4.5. 3-point bending test of pure ABS sandwich panel

The result of the 3-point bending test of the sandwich panel with 1% $CaCO_3$ contribution is given in Figure 4.6. As a result of this analysis, this simulated test sample resisted a maximum loading of 24.185 MPa.

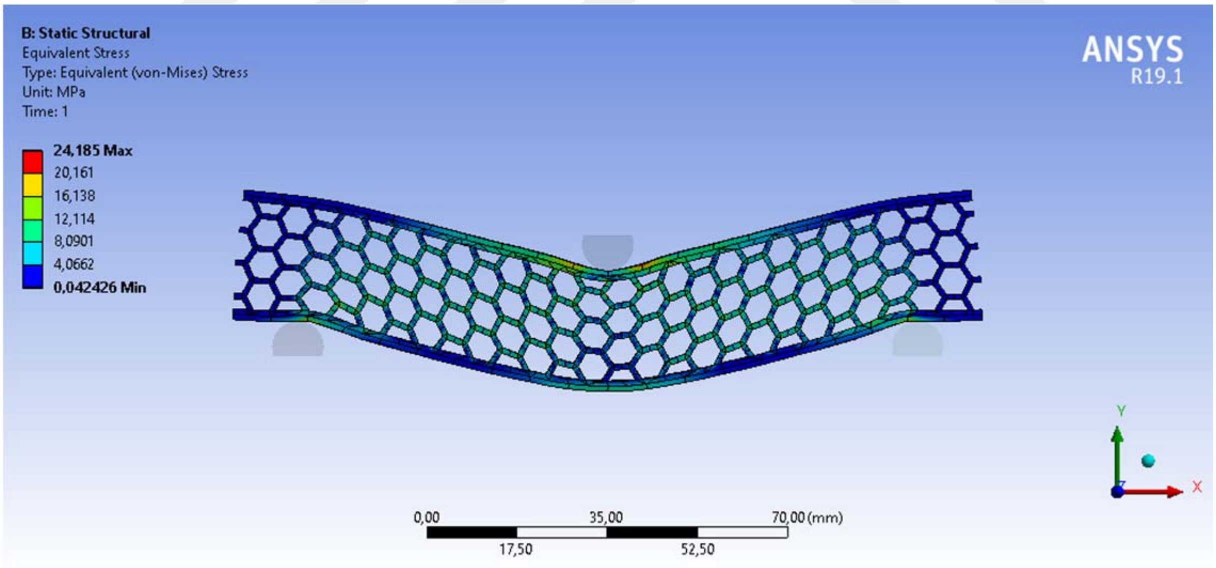

Figure 4.6. 3-point bending test of sandwich panel with 1% $CaCO_3$ additive

The result of the 3-point bending test of the sandwich panel with 2% $CaCO_3$ is given in Figure 4.7. As a result of this analysis, this simulated test sample withstood a maximum load of 30.153 MPa.

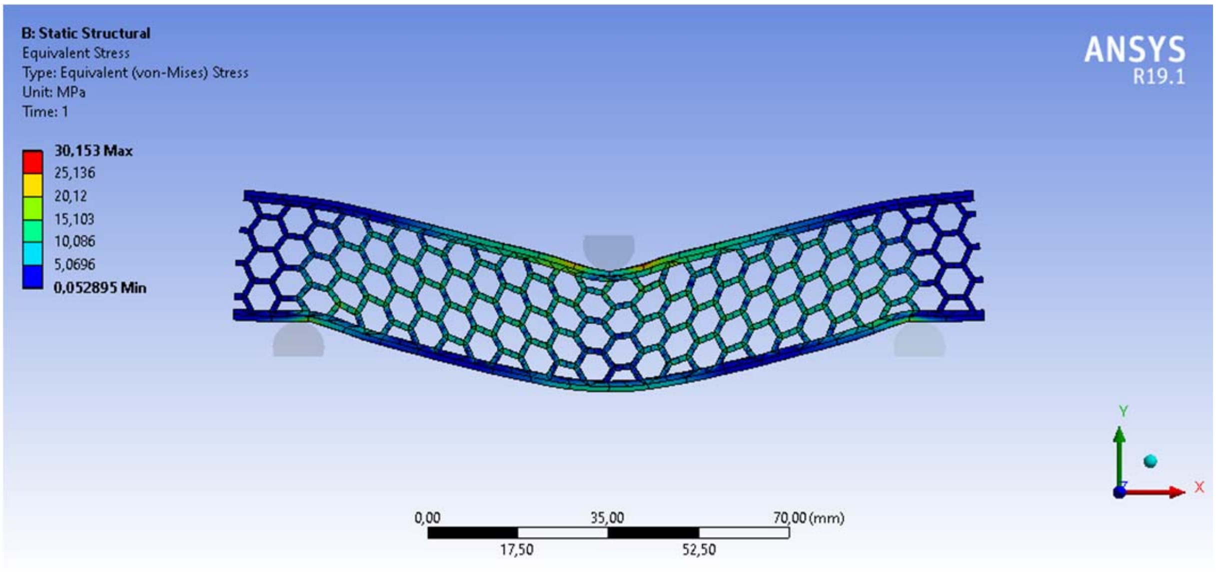

Figure 4.7. 3-point bending test of sandwich panel with 2% $CaCO_3$ additive

The result of the 3-point bending test of the sandwich panel with 3% $CaCO_3$ is given in Figure 4.8. As a result of this analysis, this simulated test sample resisted a maximum load of 33.503 MPa.

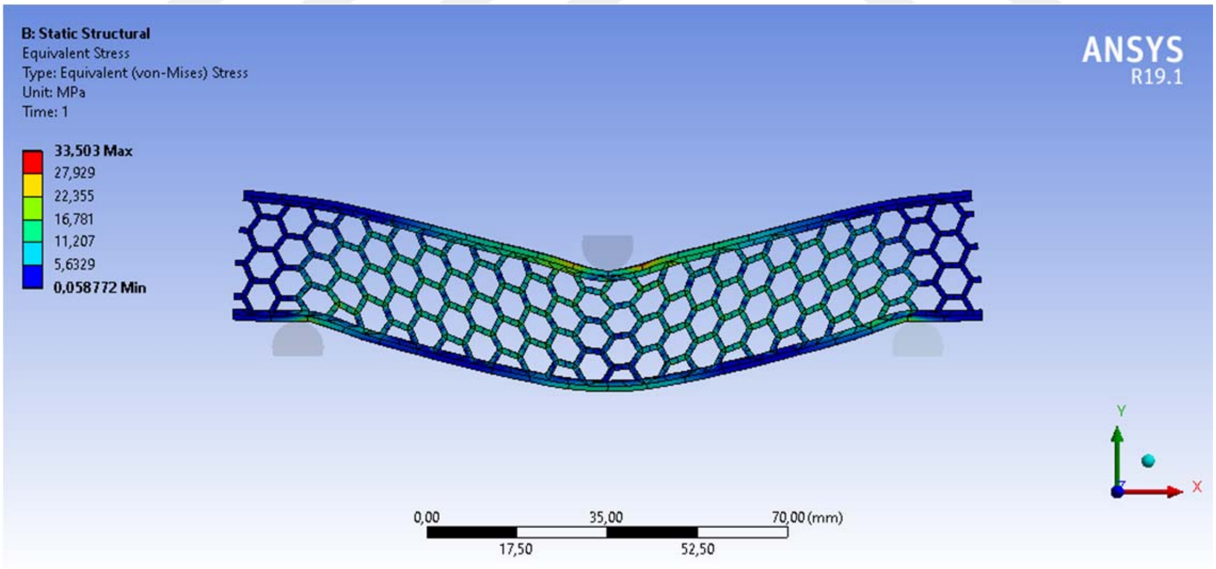

Figure 4.8. 3-point bending test of sandwich panel with 3% $CaCO_3$ additive

The result of the 3-point bending test of the sandwich panel with 5% $CaCO_3$ additive is given in Figure 4.9. As a result of this analysis, this simulated test sample resisted a maximum load of 19.683 MPa.

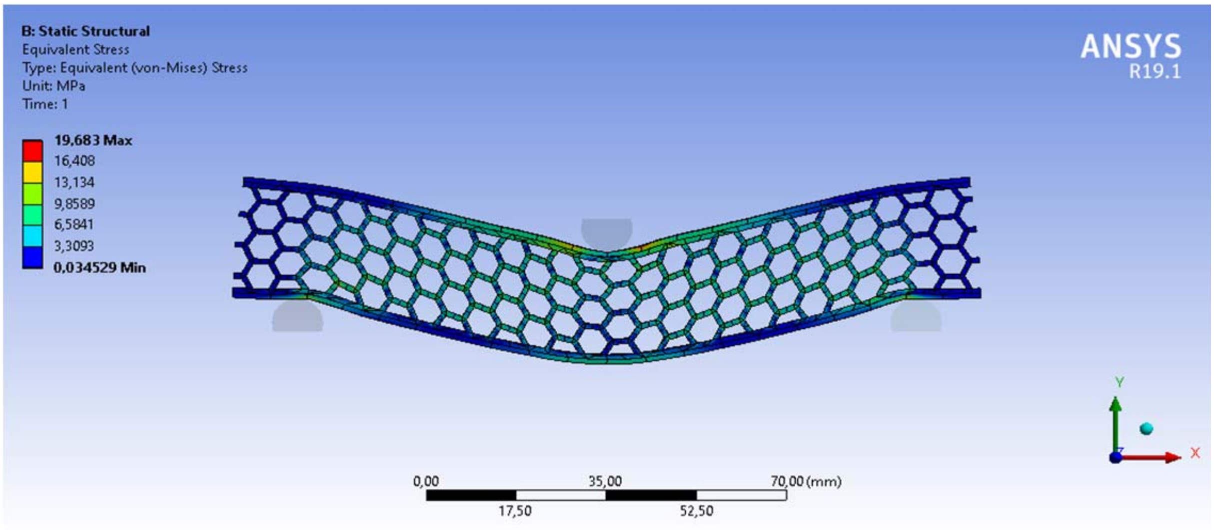

Figure 4.9. 3-point bending test of sandwich panel with 5% $CaCO_3$ additive

4.3.2. Finite Element Analysis Compression Test Findings

The compression bending test result of the sandwich panel modeled using pure ABS material properties is given in Figure 4.10. As a result of this analysis, this simulated test sample resisted a maximum load of 1.1129 MPa.

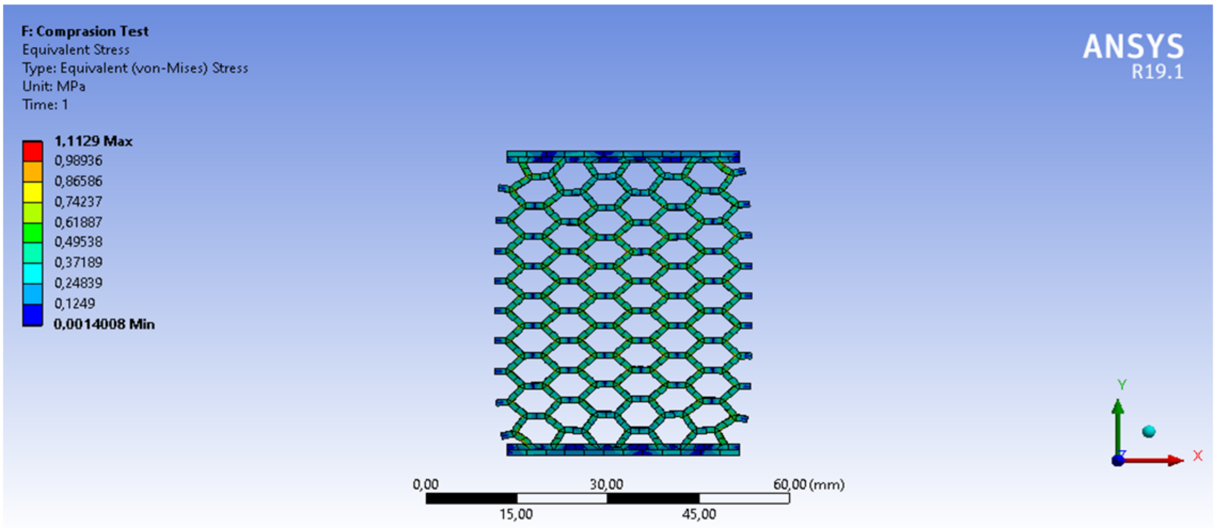

Figure 4.10. Compression bending test of sandwich panel with pure ABS

Compression bending test result of sandwich panel with 1% $CaCO_3$ additive ratio is given in Figure 4.11. As a result of this analysis, this simulated test sample withstood a maximum load of 1.5524 MPa.

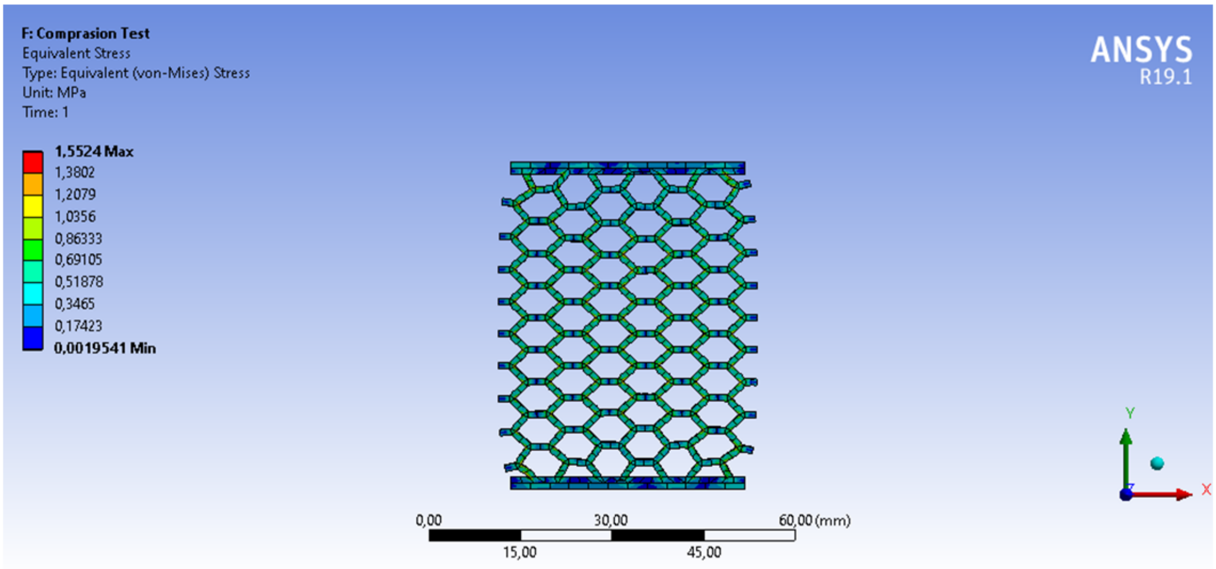

Figure 4.11. Compression bending test of sandwich panel with 1% $CaCO_3$ additive

Compression bending test result of sandwich panel with 2% $CaCO_3$ additive is given in Figure 4.12. As a result of this analysis, this simulated test sample resisted a maximum load of 1.9382 MPa.

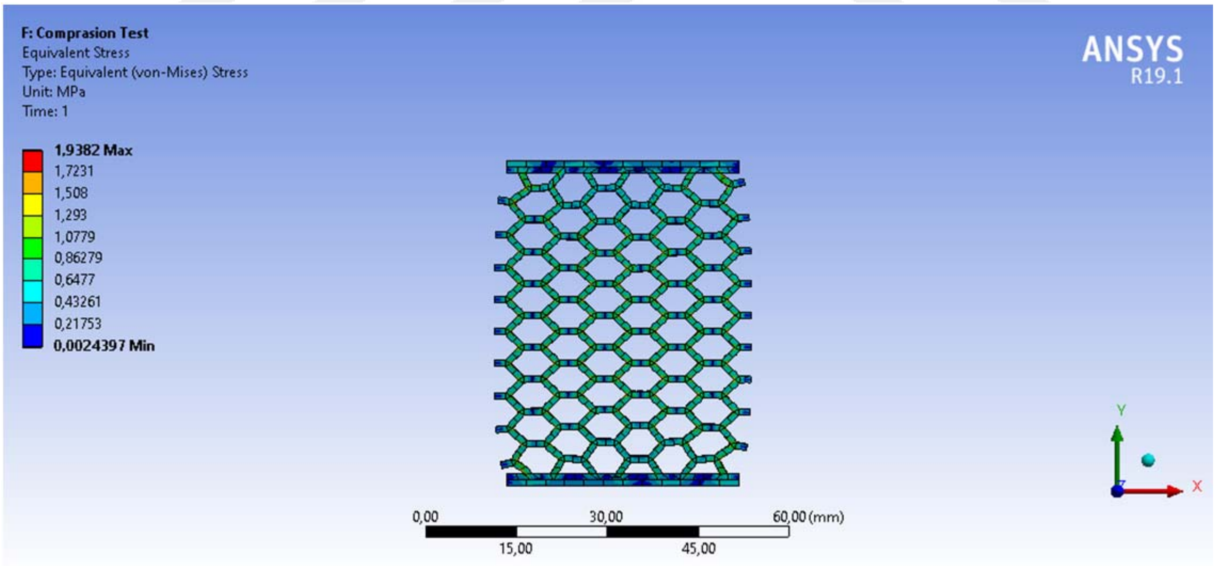

Figure 4.12. Compression bending test of sandwich panel with 2% $CaCO_3$ additive

Compression bending test result of sandwich panel with 3% $CaCO_3$ additive ratio is given in Figure 4.13. As a result of this analysis, this simulated test sample resisted a maximum load of 2.133 MPa.

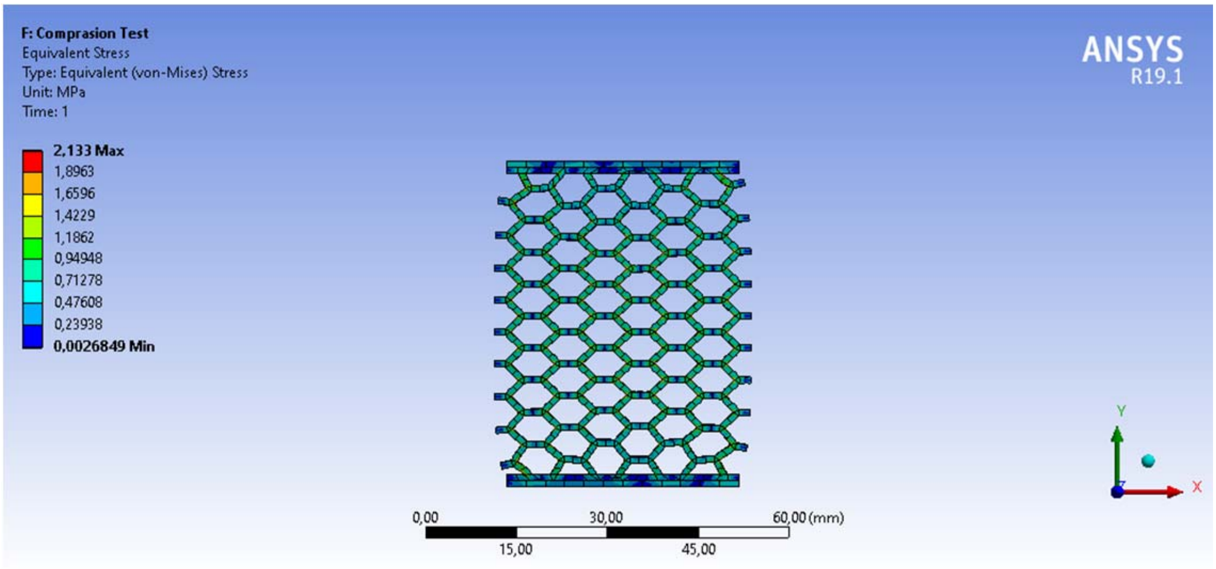

Figure 4.13. Compression bending test of sandwich panel with 3% $CaCO_3$ additive

Compression bending test result of sandwich panel with 5% $CaCO_3$ additive ratio is given in Figure 4.14. As a result of this analysis, this simulated test sample resisted a maximum load of 1.2427 MPa.

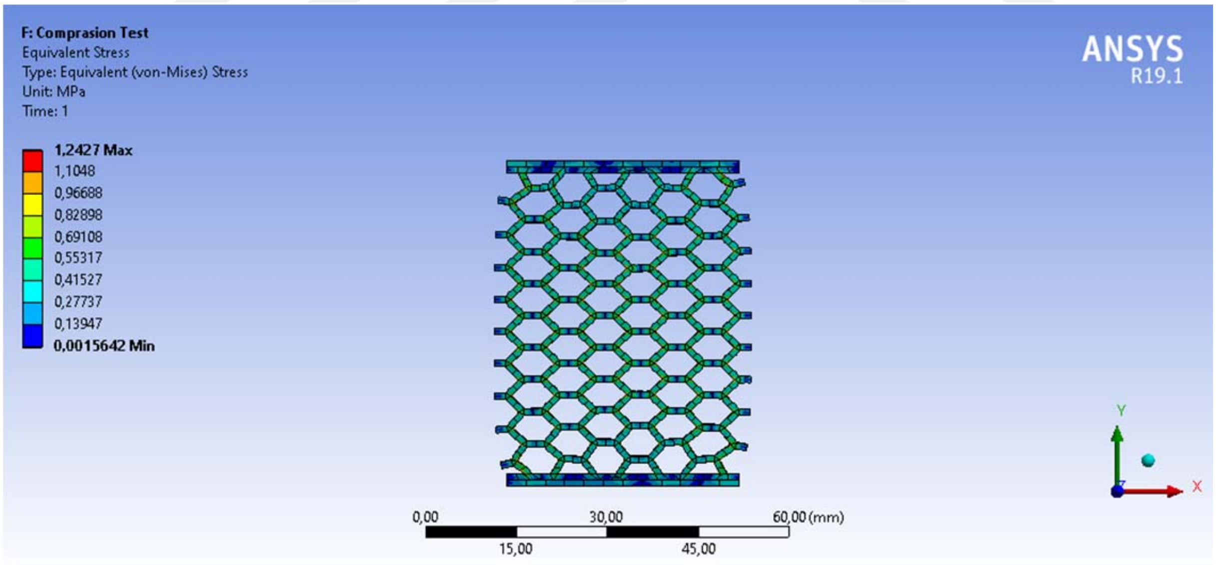

Figure 4.14. Compression bending test of sandwich panel with 5% $CaCO_3$ additive

4.4. Comparison of Test Results and Finite Element Analysis Results

As a result of this thesis, first of all, experimental tests were applied. The results of the experimental tests were obtained and presented. Then, numerical modeling was done and the tests were simulated in the computer environment. Finite element method was applied with computer aided modeling. The results of the numerical tests were determined and presented. In this section, the results of the experimental tests and the results of the numerical tests are compared.

4.4.1. 3-Point Bending Test Finite Element Analysis Results

The maximum bending stress was calculated using the experimental 3-point bending test results. Equation 4 was used when calculating the maximum bending stress. Numerical test results give the maximum bending stress. Experimental 3-point bending test results and numerical 3-point bending test results are compared in the table. In addition, the error rate is given in the Table 4.2. Results showed that these two methods confirmed each other.

Table 4.2 Comparison of 3-point bending test results

Additive Ratio	Experimental (Maximum Bending Stress), MPa	ANSYS (Maximum Bending Stress), MPa	Error Rate
Pure ABS	17.41	17.79	-0,00022
%1	24.18	24.18	0,00000
%2	30.22	30.15	0,00002
%3	33.23	33.50	-0,00008
%5	19.34	19.68	-0,00018

4.4.2. Finite Element Analysis Compression Test Results

The maximum compressive stress was calculated using the experimental compression test results. Equation 5 was used when calculating the maximum compressive stress. Numerical test results give the maximum compressive stress. Experimental compression test results and numerical compression test results are compared in the table. Also, the error rate is given in the table. The results revealed that these two methods confirmed each other.

Table 4.3 Compression test results

Additive Ratio	Experimental (Compressive stress), MPa	ANSYS (Compressive stress), MPa	Error Rate
Pure ABS	1.11	1.11	0
%1	1.55	1.55	0
%2	1.93	1.93	0
%3	2.13	2.13	0
%5	1.24	1.24	0

5. CONCLUSIONS

In this thesis, firstly pure ABS and then 1%, 2%, 3%, 5% $CaCO_3$ nanoparticle added ABS filaments were produced. With these filaments, sandwich panel cores in honeycomb geometry were produced in a double extruder 3D printer. Then, sandwich panel exterior surfaces were produced as composite plates by vacuum infusion method using unidirectional carbon fiber fabric and epoxy. The core and composite outer surfaces produced were combined with structural adhesive and test samples in the form of sandwich panels were obtained. After the tensile, compression and three-point bending tests, the effect of nanoparticle additive on the strength properties of sandwich panels was investigated. In addition, finite element analysis of the samples was also carried out. The data obtained from the analysis and the results obtained from the experiments were compared. As a result of this thesis study, it was seen that the $CaCO_3$ additive ratio directly affects the strength. It has been observed that the $CaCO_3$ additive added to ABS plastic up to 3% increases the strength. It was observed that the material added after 3% nanoparticle addition decreased the strength due to the increase in brittleness.

The results of the experimental 3-point bending test show that the sandwich panel produced using 3% $CaCO_3$ added ABS filament showed the highest strength and withstood a maximum load of 1518.504 N. The maximum bending stress was calculated using the data.

As a result of the 3-point bending test of the 3% nanoparticle added sample, it was determined that the maximum bending stress was 33.23 MPa. Numerical test results also revealed that ABS filament with 3% $CaCO_3$ nanoparticle added showed the highest strength in 3-point bending test. As a result of the numerical 3 point bending test (ANSYS 3 point bending test) using the material properties of ABS filament with 3% $CaCO_3$ nanoparticle doped, it was determined that the Maximum Bending Stress was 33.50 MPa. The strength of ABS plastic with 3% nanoparticle addition has increased significantly compared to pure ABS. Bending Stress increased 90% from 17.41 MPa to 33.23 MPa.

The results of the experimental compression test show that the sandwich panel produced using 3% $CaCO_3$ added ABS filament showed the highest strength and withstood a maximum load of 3077.28 N. The compression stress was calculated using the data. As a result of the compression test of the 3% nanoparticle added sample, it was determined that the compression stress was 2.13 MPa. Numerical test results also revealed that ABS filament with 3% $CaCO_3$ nanoparticle added showed the highest strength in compression test.

As a result of the numerical compression test (ANSYS compression test) using the material properties of 3% $CaCO_3$ nanoparticle added ABS filament, the compression stress was determined to be 2.13 MPa. The strength of ABS plastic with 3% nanoparticle addition has increased significantly compared to pure ABS. Compressive stress increased by more than 91% from strength of 1.11 MPa to 2.13 MPa.

The closeness of the experimental and numerical results showed that using the numerical method would give accurate results.

6. RECOMMENDATIONS

The consistency in the results of this study has guided future studies. It has been shown that performing experiments with the numerical method without the need for experimental work will reveal sufficient results.

It will be very useful to carry out optimization studies of sandwich panels used in all areas of the industry today, where costs are high and time is constrained, using numerical methods. The effect of additives with different material properties on strength can be observed by using the methods in these studies.

By adding $CaCO_3$ material, which is the subject of this study, to other materials other than ABS material, its effect on strength can be observed. The effect of geometries on strength can be observed by using core materials with geometries other than honeycomb. In addition, the effect of both the angles and the number of layers of the composite plates on the strength can be modeled and observed numerically.

REFERENCES

Abbood, I. S., aldeen Odaa, S., Hasan, K. F., & Jasim, M. A. (2021). Properties evaluation of fiber reinforced polymers and their constituent materials used in structures–A review. *Materials Today: Proceedings*, *43*, 1003-1008.

Ahmad, S., Zhang, J., Feng, P., Yu, D., Wu, Z., & Ke, M. (2020). Processing technologies for Nomex honeycomb composites (NHCs): A critical review. *Composite Structures*, *250*, 112545.

Ahmed, W., Ahmed, S., Alnajjar, F., & Zaneldin, E. (2021). Mechanical performance of three-dimensional printed sandwich composite with a high-flexible core. *Proceedings of the Institution of Mechanical Engineers, Part L: Journal of Materials: Design and Applications*, *235*(6), 1382-1400.

Al Omari, M. M. H., Rashid, I. S., Qinna, N. A., Jaber, A. M., & Badwan, A. A. (2016). Calcium carbonate. *Profiles of drug substances, excipients and related methodology*, *41*, 31-132.

Araya-Calvo, M., López-Gómez, I., Chamberlain-Simon, N., León-Salazar, J. L., Guillén-Girón, T., Corrales-Cordero, J. S., & Sánchez-Brenes, O. (2018). Evaluation of compressive and flexural properties of continuous fiber fabrication additive manufacturing technology. *Additive Manufacturing*, *22*, 157-164.

Audibert, C., Andréani, A. S., Lainé, É., & Grandidier, J. C. (2019). Discrete modelling of low-velocity impact on Nomex® honeycomb sandwich structures with CFRP skins. *Composite Structures*, *207*, 108-118.

Bai, R., Guo, J., Lei, Z., Liu, D., Ma, Y., & Yan, C. (2019). Compression after impact behavior of composite foam-core sandwich panels. *Composite Structures*, *225*, 111181.

Banhart, J., & Seeliger, H. W. (2008). Aluminium foam sandwich panels: manufacture, metallurgy and applications. *Advanced Engineering Materials*, *10*(9), 793-802.

Belouettar, S., Abbadi, A., Azari, Z., Belouettar, R., & Freres, P. (2009). Experimental investigation of static and fatigue behaviour of composites honeycomb materials using four point bending tests. *Composite Structures*, *87*(3), 265-273.

Bulut, M. (2017). Mechanical characterization of Basalt/epoxy composite laminates containing graphene nanopellets. *Composites Part B: Engineering*, *122*, 71-78.

Choupani, N. (2008). Experimental and numerical investigation of the mixed-mode delamination in Arcan laminated specimens. *Materials Science and Engineering: A*, *478*(1-2), 229-242.

Christy, A., Purohit, R., Rana, R. S., Singh, S. K., & Rana, S. (2017). Development and analysis of epoxy/nano SiO2 polymer matrix composite fabricated by ultrasonic vibration assisted processing. *Materials Today: Proceedings*, *4*(2), 2748-2754.

Crupi, V., & Montanini, R. (2007). Aluminium foam sandwiches collapse modes under static and dynamic three-point bending. *International Journal of Impact Engineering*, *34*(3), 509-521.

Crupi, V., Epasto, G., & Guglielmino, E. (2012). Collapse modes in aluminium honeycomb sandwich panels under bending and impact loading. *International Journal of Impact Engineering*, *43*, 6-15.

Çava K. (2019) "Investigation of the usage characteristics of FDM type 3 dimensional printer thermoplastic honeycomb / auxetic core material design, production and sandwich composites" *Karadeniz Teknik Üniversitesi / Fen Bilimleri Enstitüsü / Metalurji ve Malzeme Mühendisliği Ana Bilim Dalı, 67*

Davalos, J. F., Qiao, P., Xu, X. F., Robinson, J., & Barth, K. E. (2001). Modeling and characterization of fiber-reinforced plastic honeycomb sandwich panels for highway bridge applications. *Composite structures*, *52*(3-4), 441-452.

De Dios Rodriguez-Ramirez, J., Castanié, B., & Bouvet, C. (2018). Experimental and numerical analysis of the shear nonlinear behaviour of Nomex honeycomb core: Application to insert sizing. *Composite Structures*, *193*, 121-139..

Ding, K. W., Wang, G., & Yin, W. Y. (2013). Application of composite sandwich panels in construction engineering. In *Applied Mechanics and Materials* (Vol. 291, pp. 1172-1176). Trans Tech Publications Ltd.

Essabir, H., Bensalah, M. O., Rodrigue, D., & Bouhfid, R. (2017). A comparison between bio- and mineral calcium carbonate on the properties of polypropylene composites. *Construction and Building Materials*, *134*, 549-555.

Flores-Johnson, E. A., & Li, Q. M. (2010). Indentation into polymeric foams. *International Journal of Solids and Structures*, *47*(16), 1987-1995.

Foo, C. C., Chai, G. B., & Seah, L. K. (2007). Mechanical properties of Nomex material and Nomex honeycomb structure. *Composite structures*, *80*(4), 588-594.

Georgescu, M., & Ungureanu, V. (2014). Stabilisation of continuous Z-purlins by sandwich panels: Full scale experimental approach. *Thin-Walled Structures*, *81*, 242-249.

Godoi, F. C., Prakash, S., & Bhandari, B. R. (2016). 3d printing technologies applied for food design: Status and prospects. *Journal of Food Engineering*, *179*, 44-54.

Gupta, N., Weber, C., & Newsome, S. (2012). Additive manufacturing: status and opportunities. *Science and Technology Policy Institute, Washington*.

Han, B., Qin, K. K., Yu, B., Zhang, Q. C., Chen, C. Q., & Lu, T. J. (2015). Design optimization of foam-reinforced corrugated sandwich beams. *Composite Structures*, *130*, 51-62.

Han, B., Qin, K., Yu, B., Wang, B., Zhang, Q., & Lu, T. J. (2016). Honeycomb–corrugation hybrid as a novel sandwich core for significantly enhanced compressive performance. *Materials & Design*, *93*, 271-282.

Han, B., Wang, W., Zhang, Z., Zhang, Q., Jin, F., & Lu, T. (2016). Performance enhancement of sandwich panels with honeycomb–corrugation hybrid core. *Theoretical and Applied Mechanics Letters*, *6*(1), 54-59.

He, M., & Hu, W. (2008). A study on composite honeycomb sandwich panel structure. *Materials & Design*, *29*(3), 709-713.

Heimbs, S., Schmeer, S., Middendorf, P., & Maier, M. (2007). Strain rate effects in phenolic composites and phenolic-impregnated honeycomb structures. *Composites Science and Technology*, *67*(13), 2827-2837.

Hipke, T., Hohlfeld, J., & Rybandt, S. (2014). Functionally aluminum foam composites for building industry. *Procedia Materials Science*, *4*, 133-138.

Hou, Y., Tai, Y. H., Lira, C., Scarpa, F., Yates, J. R., & Gu, B. (2013). The bending and failure of sandwich structures with auxetic gradient cellular cores. *Composites Part A: Applied Science and Manufacturing*, *49*, 119-131.

Kabir, S. F., Mathur, K., & Seyam, A. F. M. (2020). A critical review on 3D printed continuous fiber-reinforced composites: History, mechanism, materials and properties. *Composite Structures*, *232*, 111476.

Kabir, S. F., Mathur, K., & Seyam, A. F. M. (2020). A critical review on 3D printed continuous fiber-reinforced composites: History, mechanism, materials and properties. *Composite Structures*, *232*, 111476.

Kim, K. Y., & Ye, L. (2004). Interlaminar fracture toughness of CF/PEI composites at elevated temperatures: roles of matrix toughness and fibre/matrix adhesion. *Composites Part A: Applied Science and Manufacturing*, *35*(4), 477-487.

Lauwaert, M. (2008). Playing outside the box–on LEGO toys and the changing world of construction play. *History and Technology*, *24*(3), 221-237.

Li, S., Wu, Q., Zhu, H., Lin, Q., & Wang, C. (2017). Impact resistance enhancement by adding core-shell particle to epoxy resin modified with hyperbranched polymer. *Polymers*, *9*(12), 684.

Lim, S., Buswell, R. A., Le, T. T., Austin, S. A., Gibb, A. G., & Thorpe, T. (2012). Developments in construction-scale additive manufacturing processes. *Automation in construction*, *21*, 262-268.

Liu, L., Wang, H., & Guan, Z. (2015). Experimental and numerical study on the mechanical response of Nomex honeycomb core under transverse loading. *Composite Structures*, *121*, 304-314.

Liu, L., Wang, H., & Guan, Z. (2015). Experimental and numerical study on the mechanical response of Nomex honeycomb core under transverse loading. *Composite Structures*, *121*, 304-314.M. Hussain, N. Abbas, N. Zahra, U. Sajjad, and M. B. Awan(2019). Investigating the performance of GFRP/wood-based honeycomb sandwich panels for sustainable prefab building construction, *SN Appl. Sci.* 1, 875.

Marsh, G. (2010). Airbus A350 XWB update. *Reinforced plastics*, *54*(6), 20-24.

Mishra, S. R., Kumar, S., Park, A., Rho, J., Losby, J., & Hoffmeister, B. K. (2003). Ultrasonic characterization of the curing process of PCC fly ash–cement composites. *Materials Characterization*, *50*(4-5), 317-323.

Moore, J. D. (1973). Acrylonitrile-butadiene-styrene (ABS)-a review. *Composites*, *4*(3), 118-130.

Nazzi, F. (2016). The hexagonal shape of the honeycomb cells depends on the construction behavior of bees. *Scientific reports*, *6*(1), 1-6.

O'Hegarty, R., & Kinnane, O. (2020). Review of precast concrete sandwich pane

Park, Y. B., Kweon, J. H., & Choi, J. H. (2014). Failure characteristics of carbon/BMI-Nomex sandwich joints in various hygrothermal conditions. *Composites Part B: Engineering*, *60*, 213-221.

Peterson, A. M. (2019). Review of acrylonitrile butadiene styrene in fused filament fabrication: A plastics engineering-focused perspective. *Additive Manufacturing*, *27*, 363-371.

Quan, Z., Wu, A., Keefe, M., Qin, X., Yu, J., Suhr, J., ... & Chou, T. W. (2015). Additive manufacturing of multi-directional preforms for composites: opportunities and challenges. *Materials Today*, *18*(9), 503-512.

Rajaneesh, A., Zhao, Y., Chai, G. B., & Sridhar, I. (2018). Flexural fatigue life prediction of CFRP-Nomex honeycomb sandwich beams. *Composite Structures*, *192*, 225-231.

Revilla-León, M., Sadeghpour, M., & Özcan, M. (2020). A review of the applications of additive manufacturing technologies used to fabricate metals in implant dentistry. *Journal of Prosthodontics*, *29*(7), 579-593

Richard, O., West, R., Reilly, A., & Kinnane, O. (2019). Composite behaviour of fibre-reinforced concrete sandwich panels with FRP shear connectors. *Engineering Structures*, *198*, 109475.

Roy, R., Park, S. J., Kweon, J. H., & Choi, J. H. (2014). Characterization of Nomex honeycomb core constituent material mechanical properties. *Composite Structures*, *117*, 255-266.

Sales, R. D. C. M., Gusmao, S. R., Gouvea, R. F., Chu, T., Marlet, J. M. F., Candido, G. M., & Donadon, M. V. (2017). The temperature effects on the fracture toughness of carbon fiber/RTM-6 laminates processed by VARTM. *Journal of Composite Materials*, *51*(12), 1729-1741.

Sang, L., Han, S., Peng, X., Jian, X., & Wang, J. (2019). Development of 3D-printed basalt fiber reinforced thermoplastic honeycombs with enhanced compressive mechanical properties. *Composites Part A: Applied Science and Manufacturing*, *125*, 105518.

Savage, G. (2008). Composite materials technology in formula 1 motor racing. *Honda Racing F1 Team*, *91*, 92.

Savage, G. (2010). Formula 1 composites engineering. *Engineering failure analysis*, *17*(1), 92-115.

Sharaf, T., & Fam, A. (2011). Experimental investigation of large-scale cladding sandwich panels under out-of-plane transverse loading for building applications. *Journal of Composites for Construction*, *15*(3), 422-430.

Smith, P. M., & Wolcott, M. P. (2006). Opportunities for wood/natural fiber-plastic composites in residential and industrial applications. *Forest Products Journal*, *56*(3), 4.

Starke, J. (2016). Carbon composites in automotive structural applications. *EuCIA: Composites and Sustainability*.

St-Pierre, L., Deshpande, V. S., & Fleck, N. A. (2015). The low velocity impact response of sandwich beams with a corrugated core or a Y-frame core. *International Journal of Mechanical Sciences*, *91*, 71-80.

St-Pierre, L., Fleck, N. A., & Deshpande, V. S. (2015). The dynamic indentation response of sandwich panels with a corrugated or Y-frame core. *International Journal of Mechanical Sciences*, *92*, 279-289.

Sugiyama, K., Matsuzaki, R., Ueda, M., Todoroki, A., & Hirano, Y. (2018). 3D printing of composite sandwich structures using continuous carbon fiber and fiber tension. *Composites Part A: Applied Science and Manufacturing*, *113*, 114-121.

Sun, G., Huo, X., Chen, D., & Li, Q. (2017). Experimental and numerical study on honeycomb sandwich panels under bending and in-panel compression. *Materials & Design*, *133*, 154-168.

Tang, E., Zhang, X., & Han, Y. (2019). Experimental research on damage characteristics of CFRP/aluminum foam sandwich structure subjected to high velocity impact. *Journal of Materials Research and Technology*, *8*(5), 4620-4630.

Tofail, S. A., Koumoulos, E. P., Bandyopadhyay, A., Bose, S., O'Donoghue, L., & Charitidis, C. (2018). Additive manufacturing: scientific and technological challenges, market uptake and opportunities. *Materials today*, *21*(1), 22-37.

Tuncer C. (2018). $CaCO_3$, SiO2 ve Grafen Nano Partikül Katkisinin Tabakali Cam Elyaf Kompozit Malzemelerin Mekanik Özelliklerine Etkisi, 51

Wang, J., Waas, A. M., & Wang, H. (2013). Experimental and numerical study on the low-velocity impact behavior of foam-core sandwich panels. *Composite Structures*, *96*, 298-311.

Wang, X., Jiang, M., Zhou, Z., Gou, J., & Hui, D. (2017). 3D printing of polymer matrix composites: A review and prospective. *Composites Part B: Engineering*, *110*, 442-458.

Wetzel, B., Haupert, F., & Zhang, M. Q. (2003). Epoxy nanocomposites with high mechanical and tribological performance. *Composites science and technology*, *63*(14), 2055-2067.

Wetzel, B., Rosso, P., Haupert, F., & Friedrich, K. (2006). Epoxy nanocomposites–fracture and toughening mechanisms. *Engineering fracture mechanics*, *73*(16), 2375-2398.

Wohlers, T. (2012, June). Recent trends in additive manufacturing. In *Proceedings of 17th European Forum on Rapid Prototyping and Manufacturing, Paris, France*.

Wu, X., Yu, H., Guo, L., Zhang, L., Sun, X., & Chai, Z. (2019). Experimental and numerical investigation of static and fatigue behaviors of composites honeycomb sandwich structure. *Composite Structures*, *213*, 165-172.

Wu, Y., Liu, Q., Fu, J., Li, Q., & Hui, D. (2017). Dynamic crash responses of bio-inspired aluminum honeycomb sandwich structures with CFRP panels. *Composites Part B: Engineering*, *121*, 122-133.

Xie, S., Feng, Z., Zhou, H., & Wang, D. (2021). Three-point bending behavior of Nomex honeycomb sandwich panels: Experiment and simulation. *Mechanics of Advanced Materials and Structures*, *28*(18), 1917-1931.

Xu, X., Augello, R., & Yang, H. (2021). The generation and validation of a CUF-based FEA model with laser-based experiments. *Mechanics of Advanced Materials and Structures*, *28*(16), 1648-1655.

Xu, X., Bureick, J., Yang, H., & Neumann, I. (2018). TLS-based composite structure deformation analysis validated with laser tracker. *Composite Structures*, *202*, 60-65.

Xu, X., Yang, H., Augello, R., & Carrera, E. (2021). Optimized free-form surface modeling of point clouds from laser-based measurement. *Mechanics of Advanced Materials and Structures*, *28*(15), 1570-1578.

Xu, X., Yang, H., Zhang, Y., & Neumann, I. (2018). Intelligent 3D data extraction method for deformation analysis of composite structures. *Composite Structures*, *203*, 254-258.

Yan, L. L., Han, B., Yu, B., Chen, C. Q., Zhang, Q. C., & Lu, T. J. (2014). Three-point bending of sandwich beams with aluminum foam-filled corrugated cores. *Materials & Design*, *60*, 510-519.

Yan, L. L., Yu, B., Han, B., Chen, C. Q., Zhang, Q. C., & Lu, T. J. (2013). Compressive strength and energy absorption of sandwich panels with aluminum foam-filled corrugated cores. *Composites Science and Technology*, *86*, 142-148.

Yao, S. S., Jin, F. L., Rhee, K. Y., Hui, D., & Park, S. J. (2018). Recent advances in carbon-fiber-reinforced thermoplastic composites: A review. *Composites Part B: Engineering*, *142*, 241-250.

Young, D., Wetmore, N., & Czabaj, M. (2018). Interlayer fracture toughness of additively manufactured unreinforced and carbon-fiber-reinforced acrylonitrile butadiene styrene. *Additive Manufacturing*, *22*, 508-515.

Zapata, P. A., Palza, H., Díaz, B., Armijo, A., Sepúlveda, F., Ortiz, J. A., ... & Oyarzún, C. (2018). Effect of CaCO3 nanoparticles on the mechanical and photo-degradation properties of LDPE. *Molecules*, *24*(1), 126.

Zhang, H., & Weng, Y. (2021). Safety Risks of Plant Fiber/Plastic Composites (PPCs) Intended for Food Contact: A Review of Potential Hazards and Risk Management Measures. *Toxics*, *9*(12), 343.

Zhang, Q., Yang, X., Li, P., Huang, G., Feng, S., Shen, C., ... & Lu, T. J. (2015). Bioinspired engineering of honeycomb structure–Using nature to inspire human innovation. *Progress in Materials Science*, *74*, 332-400.

Zhang, Y., Liu, T., & Tizani, W. (2018). Experimental and numerical analysis of dynamic compressive response of Nomex honeycombs. *Composites Part B: Engineering*, *148*, 27-39.

Zhou, Y., Wang, Q., Guo, Y., Xu, Y., Yi, X., & Jia, Y. (2018). Effect of phenolic resin thickness on frequency-dependent dynamic mechanical properties of Nomex honeycomb cores. *Composites Part B: Engineering*, *154*, 285-291.

Yahaya M. A., D. Ruan, G. Lu, and M. S. Dargusch. (2015). Response of aluminium honeycomb sandwich panels subjected to foam projectile impact-an experimental study, *Int. J. Impact Eng*. 75, 100–109.